the plant journal

The Plant Journal (2021) **106,** 1039–1057 doi: 10.1111/tpj.15217

CsLOB1 regulates susceptibility to citrus canker through promoting cell proliferation in citrus

Xiuping Zou[1,*], Meixia Du[1], Yunuo Liu[1], Liu Wu[1], Lanzhen Xu[1], Qin Long[1], Aihong Peng[1], Yongrui He[1], Maxuel Andrade[2] and Shanchun Chen[1,*]

[1]*Citrus Research Institute, Chinese Academy of Agricultural Sciences/Southwest University, Chongqing 400712, P. R. China, and*

[2]*Brazilian Biosciences National Laboratory (LNBio), Brazilian Center for Research in Energy and Materials (CNPEM), Campinas, SP, Brazil*

Received 30 October 2020; revised 18 February 2021; accepted 23 February 2021; published online 27 February 2021.
*For correspondence (e-mail zouxiuping@cric.cn and chenshanchun@cric.cn).

SUMMARY

Citrus sinensis **lateral organ boundary 1 (CsLOB1) was previously identified as a critical disease susceptibility gene for citrus bacterial canker, which is caused by** ***Xanthomonas citri*** **subsp.** ***citri*** **(Xcc). However, the molecular mechanisms of CsLOB1 in citrus response to Xcc are still elusive. Here, we constructed transgenic plants overexpressing and RNAi-silencing of** ***CsLOB1*** **using the canker-disease susceptible 'wanjincheng' orange (*C. sinensis* Osbeck) as explants. *CsLOB1*-overexpressing plants exhibited dwarf phenotypes with smaller and thicker leaf, increased branches and adventitious buds clustered on stems. These phenotypes were followed by a process of pustule- and canker-like development that exhibited enhanced cell proliferation. Pectin depolymerization and expansin accumulation were enhanced by *CsLOB1* overexpression, while cellulose and hemicellulose synthesis were increased by *CsLOB1* silence. Whilst overexpression of *CsLOB1* increased susceptibility, RNAi-silencing of *CsLOB1* enhanced resistance to canker disease without impairing pathogen entry. Transcriptome analysis revealed that CsLOB1 positively regulated cell wall degradation and modification processes, cytokinin metabolism, and cell division. Additionally, 565 CsLOB1-targeted genes were identified in chromatin immunoprecipitation-sequencing (ChIP-seq) experiments. Motif discovery analysis revealed that the most highly overrepresented binding sites had a conserved 6-bp 'GCGGCG' consensus DNA motif. RNA-seq and ChIP-seq data suggested that CsLOB1 directly activates the expression of four genes involved in cell wall remodeling, and three genes that participate in cytokinin and brassinosteroid hormone pathways. Our findings indicate that CsLOB1 promotes cell proliferation by mechanisms depending on cell wall remodeling and phytohormone signaling, which may be critical to citrus canker development and bacterial growth in citrus.**

Keywords: citrus canker, CsLOB1, disease susceptibility, cell proliferation, cell wall, hormone, regulatory mechanism.

INTRODUCTION

Citrus canker caused by *Xanthomonas citri* subsp. *citri* (Xcc) is a severe bacterial disease affecting most of the commercially important citrus cultivars. The canker symptoms induced on sweet oranges, lemons and limes include pustule formation on the surface of leaves, stems and fruits. The pustules develop into brown corky cankers surrounded by a water-soaked margin with a yellow halo (Cernadas and Benedetti, 2009).

Pustule formation and epidermal rupture, which may facilitate pathogen release to the leaf surface for disease propagation, are a characteristic phenotype in citrus canker disease (Cernadas and Benedetti, 2009; Hu *et al.*, 2014; Pereira *et al.*, 2014). During infection, Xcc injects type III effector (T3E) proteins into the plant cell to modulate host gene expression and stimulate canker development (Brunings and Gabriel, 2003; Ference *et al.*, 2018). Among T3Es of Xcc, PthA4, which belongs to the family of transcriptional activator-like effectors, is a major virulence factor (Swarup *et al.*, 1992; Yan and Wang, 2012). The disease susceptibility gene *CsLOB1* for citrus canker is a target of PthA4 (Hu *et al.*, 2014). After being injected into the host cell, PthA4 is translocated to the cell nucleus, where it specifically binds to the effector binding element in the promoter of *CsLOB1*

to trigger its transcription, which in turn promotes pustule formation and canker development (Hu *et al.*, 2014; Li *et al.*, 2014). Notably, induced expression of *CsLOB1* driven by dexamethasone in *CsLOB1-GR* transgenic plants was associated with pustule formation in Duncan grapefruit leaves (Duan *et al.*, 2018), while CRISPR/Cas9-mediated mutation of *CsLOB1* suppressed Xcc-induced pustule formation and consequently conferred plant resistance to citrus canker (Jia *et al.*, 2017; Peng *et al.*, 2017; Jia and Wang, 2020). These results have shown that *CsLOB1* plays an essential role in citrus canker disease. However, how *CsLOB1* regulates pustule formation and subsequent canker development is still poorly understood.

CsLOB1 belongs to the *lateral organ boundaries domain* (*LBD*) family encoding a member of the plant-specific LOB domain transcription factors (Xu *et al.*, 2016; Zhang *et al.*, 2017). LBD family members are classified into two subfamilies based on the presence (class I) or absence (class II) of functional leucine-zipper-like domains, though the majority of *LBD* members, including *CsLOB1* and its orthologs *AtLBD1* and *AtLBD11* in Arabidopsis, belong to class I (Shuai *et al.*, 2002; Zhang *et al.*, 2017, 2020). LBD proteins are key regulators of plant organ development, and widely participate in molecular mechanisms that control plant growth and development (Majer and Hochholdinger, 2011; Xu *et al.*, 2016). For example, AtLBD16, AtLBD17, AtLBD18 and AtLBD29 control lateral root formation through regulating callus induction (Fan *et al.*, 2012; Xu *et al.*, 2018), meanwhile AtLBD27 and AtLBD10 participate in asymmetric microspore division in Arabidopsis (Oh *et al.*, 2010; Kim *et al.*, 2015b). Several reports also showed that LBD proteins have important functions in regulation of plant response to pest or pathogen attack: AtLBD20 negatively regulates Arabidopsis resistance to the fungal pathogen *Fusarium oxysporum* through the jasmonic acid (JA) signaling pathway (Thatcher *et al.*, 2012); AtLBD16 facilitates development of gall formation comprising the feeding structure of the root-knot nematodes (Cabrera *et al.*, 2014); BvLBD16, BvLBD18 and BvLBD29 are involved in excessive lateral root formation induced by *Beet necrotic yellow vein virus* in sugar beet (Fernando Gil *et al.*, 2018). LBD proteins seem to regulate plant susceptibility to pathogen mainly by affecting plant lateral organ development or hormone homeostasis (Fernando Gil *et al.*, 2018; Xu *et al.*, 2016). Thus, manipulation of the expression of *LBD* genes is an important strategy for plant pathogens to cause disease in their hosts.

As mentioned earlier, the function of *CsLOB1* in growth and development remains to be determined in citrus. *CsLOB1* is the closest homolog of poplar *PtaLOB1* and uncharacterized *AtLBD1* and *AtLBD11* from Arabidopsis (Hu *et al.*, 2014). Because *PtaLOB1* seems to be involved in regulation of secondary growth in poplar (Yordanov *et al.*, 2010), *CsLOB1* may have a similar role in citrus. Also, PthA4-induced expression of *CsLOB1* is associated with upregulation of a subset of plant development-related genes that includes genes mediating cell wall metabolism (Hu *et al.*, 2014; Zhang *et al.*, 2017; Duan *et al.*, 2018). Thus, it suggests that some functions of CsLOB1 in plant development favor citrus canker formation and bacterial growth. In this study, we show that ectopic expression of *CsLOB1* in the canker-disease-susceptible 'wanjincheng' orange (*Citrus sinensis* Osbeck) changes plant morphology and elicits cell proliferation through a complex molecular network that leads to susceptibility to Xcc. Also, we present a model of the regulatory mechanism by which CsLOB1 triggers citrus canker disease.

RESULTS

Expression profile of *CsLOB1* in citrus plants

Previous studies showed differential expression levels of *CsLOB1* in different tissues of citrus, and that various *LBD* genes can be induced by a diversity of stressors (Xu *et al.*, 2016). Here, we firstly investigated the expression patterns of *CsLOB1* in hormone and wounding treatments by reverse transcriptase-quantitative polymerase chain reaction (RT-qPCR) analysis. Expression of *CsLOB1* was significantly upregulated by NAA (α-naphthyl acetic acid) and wounding induction (Figure 1a,b), but not obviously affected by zeatin (ZT), brassinolide (BL), gibberellin (GA) or abscisic acid (ABA) hormones (Figure S1). To investigate the tissue-specific expression of *CsLOB1*, the *CsLOB1* promoter (Peng *et al.*, 2017) was cloned upstream to the GUS (β-glucuronidase) reporter gene, and the resultant construct was introduced into 'wanjincheng' orange, which is a canker-susceptible cultivar. GUS histochemical staining indicated that the *CsLOB1* promoter activity was consistently localized in leaf, root and stem, also stronger signals were found in stomata, epidermal tissue and following several layers of the phloem (Figure 1c).

Overexpression of *CsLOB1* changes morphological traits in 'wanjincheng' orange

To understand functions of *CsLOB1* in citrus development, we constructed two vectors *pOLOB1* and *pDLOB1* using the *Cauliflower mosaic virus* 35S (*CaMV 35S*) promoter as regulatory sequence (Figure S2). These two constructs were introduced into 'wanjincheng' orange via Agrobacterium-mediated epicotyl transformation. Transgenic plants transformed with *pOLOB1* showed overexpression of *CsLOB1*, while transgenic plants transformed with *pDLOB1* expressed a hairpin double-stranded RNA for *CsLOB1* to induce sequence-specific RNA silencing. Based on RT-qPCR analysis, overexpression (O#) and silencing (D#) of *CsLOB1* were confirmed in seven and eight transgenic plants, respectively (Figure S2). All the transgenic plants were grown in a greenhouse, and their phenotypes

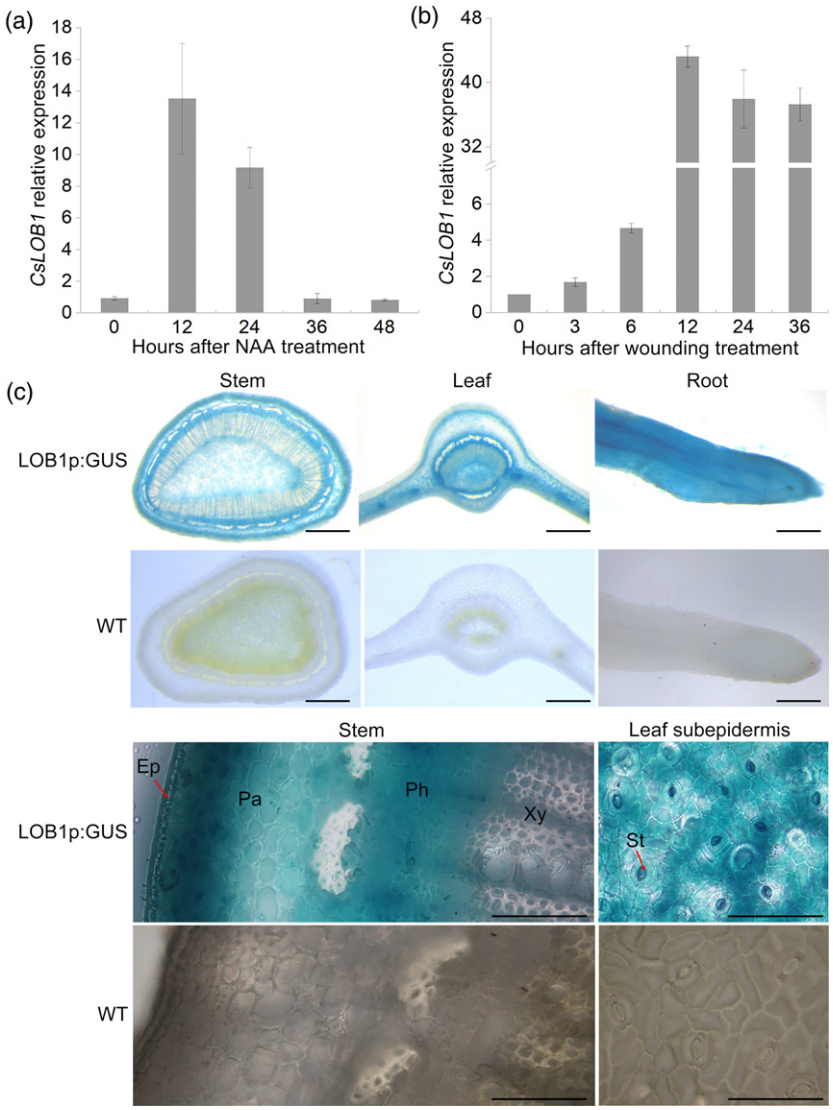

Figure 1. Expression characteristics of *CsLOB1* in 'wanjincheng' orange.
(a, b) *CsLOB1* expression induced by α-naphthyl acetic acid (NAA) (a) and wounding (b) in leaf. *CsLOB1* expressions in treated leaf were determined by reverse transcriptase-quantitative polymerase chain reaction (RT-qPCR). NAA- and wounding-induced expression levels were calculated by comparing with mock and the wounding treatment at 0 h, respectively.
(c) Expression characteristics of the *CsLOB1* promoter in transgenic 'wanjincheng' orange. Using GUS (β-glucuronidase) as reporter gene, the tissue expression pattern of the promoter was visualized by GUS histochemical staining. Scale bar: 0.2 mm. WT, wild-type. LOB1p:GUS, transgenic 'wanjincheng' orange carrying CsLOB1 promoter fused to *gusA* reporter gene. Ep, epidermis; Pa, parenchyma; Ph, phloem; Xy, xylem; St, stomata.

were investigated. During 4 years of greenhouse cultivation, most transgenic plants overexpressing *CsLOB1* displayed dwarfism phenotypes with reduced plant stature, increased branching, rough bark, and small-thick-and-upward curled leaves, compared with the wild-type (WT) control (Figures 2a and S3–S5). In *CsLOB1*-silenced plants, no visibly dwarfism phenotypes were detected (Figures S3 and S4), although the transverse diameter of leaf was shortened, and leaf area decreased compared with WT control (Figure S5). Next, we investigated the development of transgenic plants by grafting onto *Citrus junos* Sieb. ex Tanaka rootstock in a greenhouse. After 6 months, the survival rate analysis of grafted transgenic lines showed that various *CsLOB1*-overexpressing plants died, but *CsLOB1*-silenced lines had a development similar to the WT plants (Table S1). These data revealed that overexpression of *CsLOB1* severely impaired citrus plant development.

Overexpression of *CsLOB1* in 'wanjincheng' orange led to the development of many adventitious buds or callus-like bulges clustered on stems, especially in the axillary bud primordium, whereas these phenotypes were not observed in both *CsLOB1*-silenced and WT plants

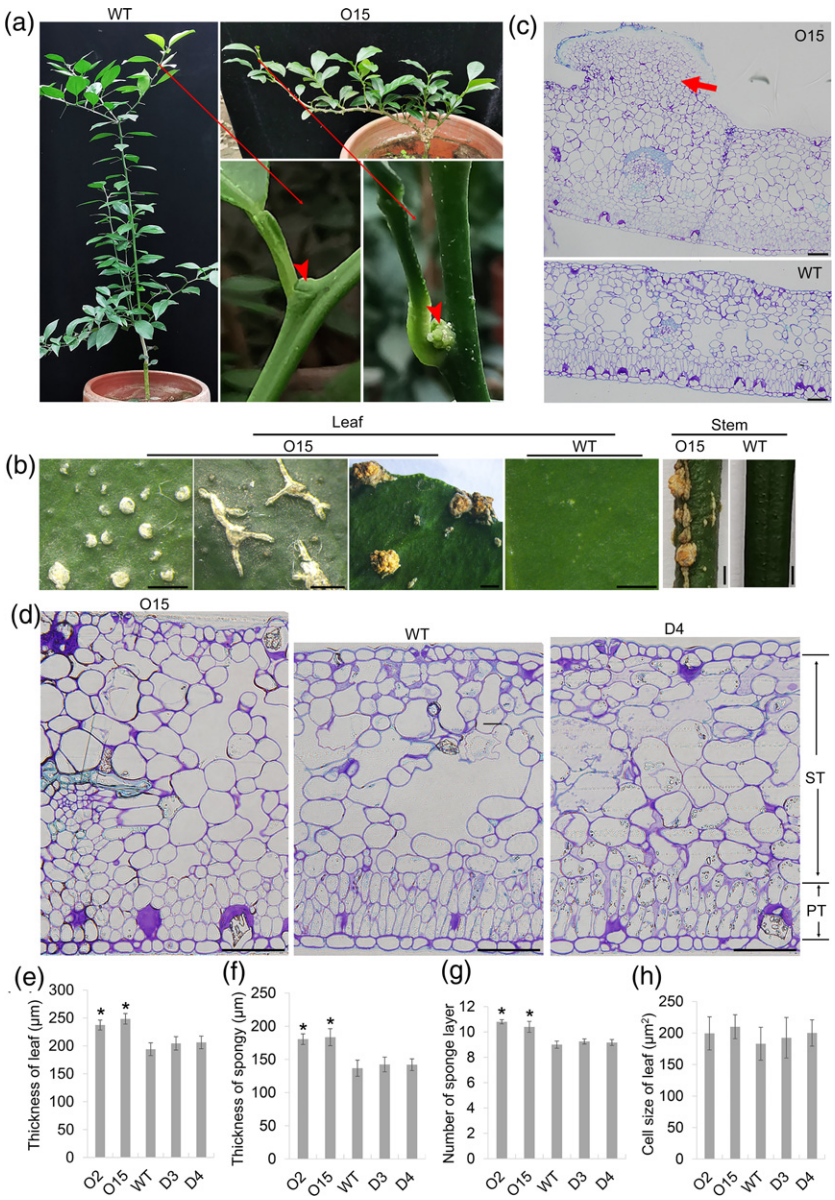

Figure 2. Phenotype characteristics of *CsLOB1*-overexpressing transgenic 'wanjincheng' orange.
(a) The dwarf phenotype of the 2-year-old O15 line in a greenhouse. It is noted that adventitious callus-like bulges (red arrowheads) appeared in the axillary bud primordium.
(b) Pustule- and canker-like development in the O15 line.
(c) Microscopic observation of cell proliferation (red arrow) elicited by *CsLOB1* overexpression in leaf from the O15 line.
(d) Microscopic observation of cellular change in fully mature leaf from transgenic plants.
The thickness (e) of leaf and spongy tissue (f), number of sponge layers (g) and cell size of leaf (h) in transgenic plants were evaluated using 10 leaves per line. Values are expressed as means ± standard deviation of three independent tests. *on top of the bars represent significant differences from WT controls based on Duncan's test ($P < 0.05$). In (c) and (d), the slides were stained with 0.01% aniline blue. O2 and O15, transgenic lines overexpressing *CsLOB1*; WT, wild-type; D3 and D4, transgenic lines RNAi-silencing *CsLOB1*; ST, spongy tissue; PT, palisade tissue. In (b), scale bar: 1 mm; in (c) and (d), scale bar: 50 μm.

(Figures 2a and S6). Also, formation of numerous bulges was detected in the leaves of *CsLOB1*-overexpressing plants (Figures 2b, S6 and S7). At the initial stage of development, bulges were small and white and similar to pustules in the early infection by Xcc, then they became bigger and grew into brown corky bulges that resembled volcano-like lesions at the later stage of citrus canker (Figures 2b and S6–S8). Microscopic observation clearly revealed that cell proliferation occurred in the bulges (Figure 2c). To confirm this result, morphology of leaf tissues from transgenic plants was further investigated. As shown in Figure 2(d,e), the leaf of *CsLOB1*-overexpressing plants

was thicker than *CsLOB1*-silenced and WT plants, which did not display any difference in leaf thickness between each other. The change of leaf thickness in *CsLOB1*-overexpressing plants was mainly due to an increased number of spongy mesophyll cells (Figure 2f,g). There was no significant difference in cell size among the three genotypes (Figure 2d,h). Additionally, palisade mesophyll cells in *CsLOB1*-overexpressing plants became short and irregular, resulting in disappearance of the classic palisade structure with two layers of cells, compared with WT plants (Figure 2d). Gene expression analysis showed that *CsLOB1* had higher expression levels in both bulge-like leaf tissues and adventitious buds when compared with that in WT and normal transgenic tissues (Figure S9). Our data reinforce the evidence that CsLOB1 positively regulates cell proliferation in citrus.

Evaluation of susceptibility to citrus canker disease in transgenic plants

One-year-old transgenic and WT plants growing in a greenhouse were evaluated for susceptibility to Xcc using the pinprick inoculation (Peng *et al.*, 2017). The test showed that the diseased areas in *CsLOB1*-overexpressing and -silenced plants were significantly larger and smaller than WT plants, respectively (Figure S10). Among these lines, the *CsLOB1*-overexpressing lines O2 and O15 had very large lesions, while the *CsLOB1*-silenced lines D3 and D4 had very small lesions (Figures 3a,b and S10). The disease severity on leaves of the O2 and O15 lines was about twofold increased, while in the D3 and D4 lines it was threefold reduced (Figure 3c). The canker susceptibility levels of these four lines were also confirmed by infiltration assay (Figure S11). After infiltration, Xcc growth was also evaluated and it displayed a faster growth rate in *CsLOB1*-overexpressing lines after 5 days post-inoculation (dpi), whereas a significant slower growth rate was observed in *CsLOB1*-silenced lines when compared with WT plants (Figure 3d). RT-qPCR analysis showed that the Xcc-induced expression levels of *CsLOB1* in RNAi lines were remarkedly lower than that of the WT plant after the inoculation period (Figure S12). Accordingly, these data indicate that *CsLOB1* promotes the susceptibility to *X. citri* subsp. *citri* in 'wanjincheng' orange. The O2, O15, D3 and D4 transgenic lines were used in the following experiments.

***CsLOB1* does not affect pathogen entry into the leaf apoplast through stomata**

Xcc enters host plant tissues mainly through stomates (Graham *et al.*, 2004). Because tissue-specific expression analysis displayed that *CsLOB1* was strongly expressed in stomata (Figure 1c), we further investigated the effect of *CsLOB1* expression on stomata development and stomatal susceptibility. The anatomical analysis demonstrated alterations in stomatal apparatus of transgenic plants (Figure S13; Table S2). Compared with WT and RNAi transgenic plants, the *CsLOB1*-overexpressing plants showed an enlarged stomatal opening (Figure S13). We noted that the keratinous protuberance outside the stomatal guard cell wall was thinner and shorter in *CsLOB1*-overexpressing plants than that in WT plants, while in RNAi transgenic plants it became thicker and longer, which led to a change in size of stomata opening (Figure S13). To investigate the effects of these changes on stomatal susceptibility, we assessed the levels of stomatal susceptibility to Xcc in transgenic plants using spray inoculation (Yang *et al.*, 2011). The numbers of canker lesions in inoculated leaves of *CsLOB1*-overexpressing and RNAi transgenic plants were significantly elevated and reduced, respectively, compared with that observed in WT plants at 30 dpi (Figure 3e–g). Moreover, we tested whether there was a relation between the number of observed lesions and number of pathogens that entered the leaf mesophyll through the stomata in a specific period of time. This assay was based on a pathogen entry assay described by Su *et al.* (2017). Our results indicated that the number of bacteria that entered into the leaf interior of the transgenic plants had no significant difference compared with those observed on WT plants at 1 h after Xcc inoculation (Figure 3h). Thus, *CsLOB1* might not be involved in regulation of pathogen entry into the leaf apoplast through stomata during early infection.

Transcriptome profiling of CsLOB1-regulated genes

To explore molecular mechanisms involved in citrus canker susceptibility due to *CsLOB1* activation and to identify potential downstream genes that are regulated by CsLOB1, comparative transcriptional profiling of transgenic and WT plants was performed using RNA sequencing (RNA-seq) assays with three biological replicates (Data S1). Fully mature leaves from 4-year-old plants were used in the RNA-seq analysis. The overview of total reads, mapped reads and the percentage of mapped reads in each replicate are shown in Tables S3 and S4. In total, 875 and 700 genes were identified as differentially expressed genes (DEGs) in the *CsLOB1*-overexpressing O2 and O15 lines, respectively, which represented significantly more than that observed on the D3 (298 DEGs) and D4 (70 DEGs) RNAi lines, when compared with WT control plants (Figure S14; Table S5). A total of 236 out of 369 DEGs shared by the O2 and O15 lines were upregulated by *CsLOB1* overexpression (Figure S14; Data S2). To validate the RNA-seq results, expressions of 32 randomly selected DEGs were investigated by RT-qPCR. RT-qPCR analysis confirmed the expression patterns of these DEGs were similar to those observed in RNA-seq data (Figure S15). Indeed, our data showed that *CsLOB1* overexpression led to extensive transcriptional

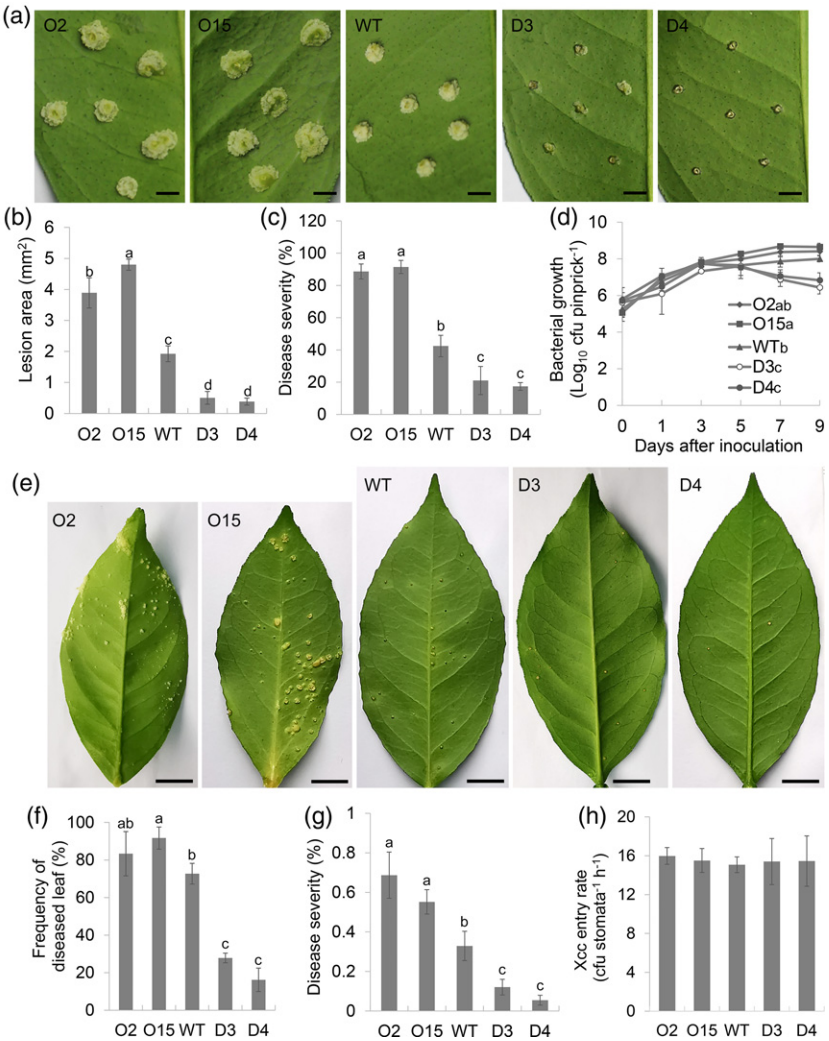

Figure 3. Evaluation of susceptibility to *Xanthomonas citri* subsp. *citri* (Xcc) in transgenic 'wanjincheng' orange.
Fully expanded leaves of transgenic and wild-type (WT) plants were inoculated with 1×10^8 CFU ml^{-1} Xcc. Citrus canker symptoms (a), diseased area (b) and disease severity (c) of leaves of transgenic lines were investigated at 9 days post-inoculation (dpi).
(d) Xcc growth in leaves of transgenic plants. The assays were performed using *in vitro* pinprick inoculation. 1 μl of 1×10^8 CFU ml^{-1} Xcc suspension was dropped onto each pinprick.
(e–g) Evaluation of stomata-mediated susceptibility to citrus canker in transgenic plants by spray inoculation. Detached leaves of transgenic and WT plants were sprayed with 1×10^8 CFU ml^{-1} Xcc. The frequency of diseased leaf and disease severity were evaluated at 30 dpi.
(h) Pathogen leaf apoplast entry assay. Xcc entry rates were calculated as Xcc number per mm^2 divided by stomatal density (Table S2) in 1 h. Values are expressed as means ± standard deviation of three independent tests. Different letters on the top of the bars and on the upper right corner represent significant differences from the WT based on Duncan's test ($P < 0.05$) at 9 dpi. O2 and O15, transgenic lines overexpressing *CsLOB1*; WT, wild-type; D3 and D4, transgenic lines RNAi-silencing *CsLOB1*. In (a) and (e), scale bar: 2 mm and 1 cm, respectively.

reprogramming compared with that in *CsLOB1*-silenced tissue.

The cellular pathways or functions affected by CsLOB1 in transgenic lines were also visualized in the MapMan tool (Thimm *et al.*, 2010). These data showed that 'cell wall', 'secondary metabolism', 'hormone metabolism', 'stress', 'RNA', 'cell', 'transport' and 'not assigned' PageMan pathways or functions were enriched in *CsLOB1*-overexpressing lines (Figure 4a; Data S3). Most notably, cell wall-related pathways (especially 'cell wall degradation', 'cell wall modification' and 'cell wall pectin esterases'), hormone pathway 'cytokinin synthesis-degradation' and 'cell.-cell division' were significantly upregulated by CsLOB1 in both the O2 and O15 lines. In addition, the pathways associated with 'misc.gluco-, galacto- and mannosidases', and 'protein.degradation.cysteine protease' were also positively affected by overexpression of *CsLOB1*. These above pathways or functions were almost unaffected by *CsLOB1* silencing. We further investigated expression profiles of the DEGs involved in both plant development and cell

signaling transduction in the O2 and O15 plants (Figure 4b; Data S4). As expected, a number of DEGs involved in cell wall degradation and modification, cell division, cell signaling and transcriptional control were significantly upregulated in these transgenic lines. Notably, all three cytokinin (CK)-related DEGs (Cs3g18090, Cs3g18100 and orange1.1t05518) shared by O2 and O15 lines showed high expression levels (log2fold change > 5) in both O2 and O15 plants (Data S4). These three genes were annotated as UDP-glucosyl transferase (UGT) family number 85A2 (UGT85A2), which is involved in N-glucosylation of CK (Šmehilová *et al.*, 2016). To sum up, our RNA-seq data indicate that *CsLOB1* overexpression significantly affects cell wall degradation and modification, cell division, and CK metabolism in citrus.

CsLOB1 positively regulates cell wall degradation and modification processes

Expression levels of all the annotated genes encoding cellulases (CL), hemicellulases (HCL), pectate lyases (PL) and polygalacturonases (PG) were significantly upregulated by CsLOB1 (Data S4). These enzymes are involved in cell wall degradation and modification processes (Barnes and Anderson, 2018). Thus, to confirm these results we evaluate these enzyme activities in transgenic plants and compared them with WT control plants. The data in Figure 5(a) showed that activities of CL and PG enzymes were significantly increased by *CsLOB1* overexpression, while HCL and PL activities were significantly decreased by *CsLOB1* silence. Interestingly, two endoxyloglucan transferase (EXGT) genes, which participate in cell wall modification (Barnes and Anderson, 2018), were also upregulated in *CsLOB1*-overexpressing lines (Data S4). However, there was no difference in EXGT activities between *CsLOB1*-overexpressing and WT plants, while its activity was significantly decreased in *CsLOB1*-silenced transgenic plants (Figure 5a). Five pectin esterase (PE) genes, which are involved in modification of cell wall pectin (Barnes and Anderson, 2018), displayed high expression levels in *CsLOB1*-overexpressing lines (Data S4). Enzymatic activity of PEs in *CsLOB1*-overexpressing and -silenced lines was significantly stronger than that in WT control, while *CsLOB1*-overexpressing lines showed the highest levels of PE activity (Figure 5a).

The CL and HCL enzymes hydrolyze cell wall cellulose and hemicellulose, respectively, and PL and PG enzymes promote pectin depolymerization (Barnes and Anderson, 2018). Analysis of the main components of the cell wall showed that protopectin and soluble pectin levels reduced more than 1.4-fold in *CsLOB1*-overexpressing lines, implying that the increased PG activities in these plants might be related to the pectin changes, while no significant variations were detected in *CsLOB1*-silenced lines (Figure 5). Nevertheless, HCL and CL contents in *CsLOB1*-silenced lines increased more than 1.6-fold, which might be due to repression of HCL enzymatic activity in these plants (Figure 5). There were no significant changes verified in *CsLOB1*-overexpressing lines. Also, four expansin genes, which are involved in cell wall loosing, were upregulated in *CsLOB1*-overexpressing lines (Data S4). Likewise, contents of expansin proteins in *CsLOB1*-overexpressing lines were markedly higher than those in RNAi and WT control plants (Figure 5b). Additionally, it was verified that lignin contents were significantly increased by overexpressing *CsLOB1* (Figure 5b). Therefore, these results imply that *CsLOB1* positively regulates cell wall degradation and modification mainly through activating pectin depolymerization and promoting the accumulation of expansin proteins.

Genome-wide binding profiles of CsLOB1 in citrus

Chromatin immunoprecipitation-sequencing (ChIP-seq) analysis was used to investigate the genome-wide binding sites of the transcriptional regulator CsLOB1 in citrus plants. These experiments were performed with two biological replicates in transgenic 'wanjincheng' orange plants expressing the construction *flag:CsLOB1*, which encodes CsLOB1 fused to FLAG-tag (Figures S16 and S17). ChIP-seq reads were mapped to the sweet orange genome (Xu *et al.*, 2013). Data quality assessment indicated that the two replicates presented good reproducibility (Figure S18). A total of 3611 and 3416 CsLOB1-binding peaks were mapped, respectively, from the two independent biological replicates (Data S5), which were mainly enriched in the promoter regions (Figures 6a and S19). Overlapping of 1066 CsLOB1-binding peaks was mapped from the two independent replicates, which represented about 31% of the total mapped peaks (Data S5). Further, motif discovery analysis revealed a 'GCGGCG' motif binding site in the putative promoter region of the sequences highly overrepresented in both biological replicates (Figure 6b). Genes that contain one or more binding sites within the 3-kb-upstream putative promoter region were considered as putative CsLOB1-targeted genes. Based on this rule, 1690 and 1635 putative CsLOB1-targeted genes were identified in the two replicates, respectively; and 565 putative CsLOB1-targeted genes were shared by the two replicates (Figure 6c; Data S6). Next, gene ontology (GO) term analysis showed that these 565 genes were enriched in different GO terms, including integral component of membrane, DNA integration, meristem initiation and cell wall organization (Figure 6d; Data S6). Among these genes, 42 transcription factor genes were detected, and many of them were involved in plant development (Data S7).

Moreover, intersection analysis of ChIP-seq and RNA-seq data highlighted 10 CsLOB1-targeted genes that were also differentially expressed in both *CsLOB1*-overexpressing lines (Figure S20a; Table 1). Notably, four CsLOB1-

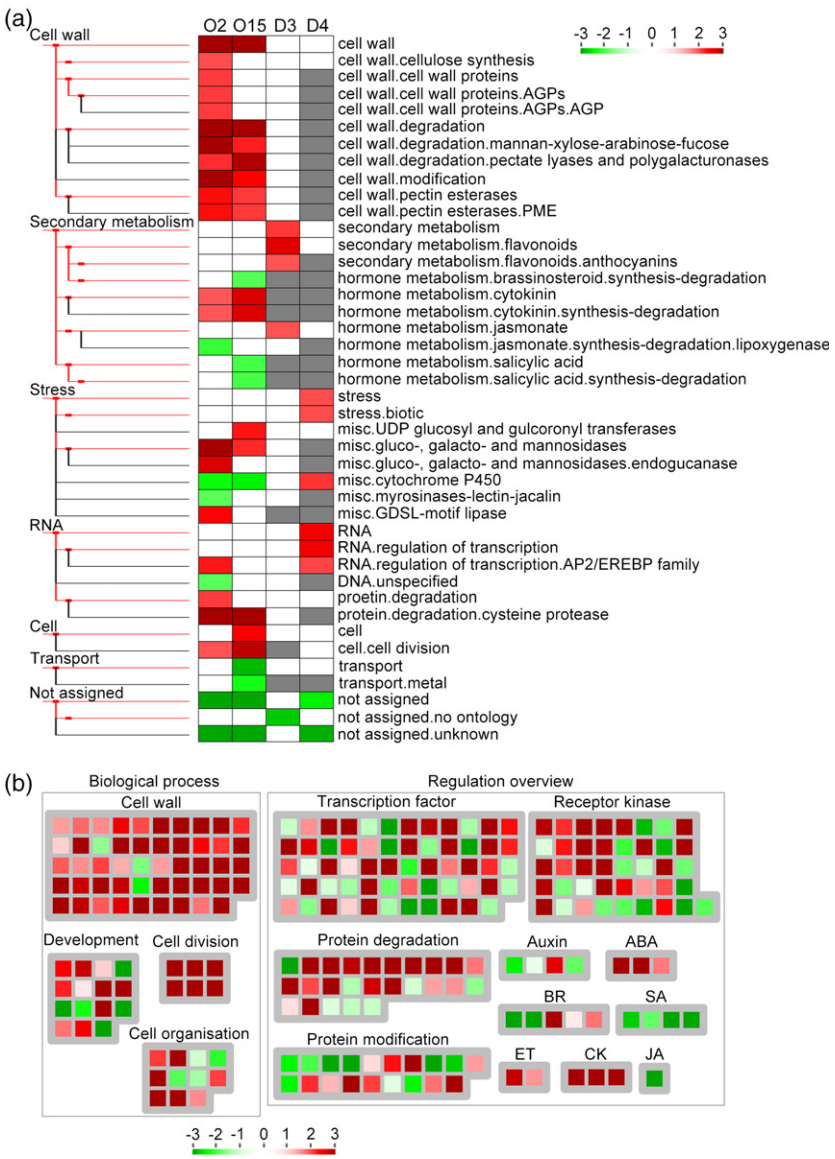

Figure 4. Ectopic expression of *CsLOB1* causes global transcriptional reprogramming in transgenic 'wanjincheng' orange.
(a) PageMan visualization of differentially represented pathways and functional categories among transgenic citrus lines. Each colored rectangular block denotes a MapMan pathway or functional category. Upregulated and downregulated categories are shown in red and green, respectively. A gray rectangular block indicates a category was not enriched. The categories differentially represented in the transgenic plants are indicated on the right.
(b) MapMan visualization of differentially expressed genes (DEGs) involved in biological process and regulation in the O15 line. Every square block indicated a gene, and significantly upregulated and downregulated genes are displayed in red and green, respectively. The scale bar represents log2 (fold-change) values. O2 and O15, transgenic lines overexpressing *CsLOB1*; WT, wild-type; D3 and D4, transgenic lines RNAi-silencing *CsLOB1*. ABA, abscisic acid; BR, brassinosteroid; SA, salicylic acid; ET, ethylene; CK, cytokinin; JA jasmonic acid.

targeted genes (Cs2g19350, Cs4g08750, Cs2g20750 and orange1.1t02719) were involved in cell wall organization, degradation and modification processes, and had significantly increased expressions in *CsLOB1*-overexpressing lines (Figure S15; Table 1). In addition, the products of two CsLOB1-targeted genes (Cs9g14190 and orange1.1t05518), which participate in brassinosteroid (BR) signal transduction and CK metabolism, respectively, were upregulated by *CsLOB1* overexpression (Figure S15; Table 1). Likewise, a putative transcription factor gene *IBH1-like 1* (Cs4g02590) that is involved in cell and organ elongation (Zhang *et al.*, 2009) was targeted and significantly upregulated by CsLOB1 (Figure S15; Table 1). In line with these findings, the expression analysis of CsLOB1-targeted genes showed that they were induced by Xcc infection in 'wanjincheng' orange (Figure S20b).

DISCUSSION

CsLOB1 triggers citrus canker development by activating cell proliferation

Activation of *CsLOB1* expression promotes pustule formation (Hu *et al.*, 2014; Duan *et al.*, 2018). However, the detailed molecular mechanism regulating pustule formation by CsLOB1 is still unclear. Indeed, LBD proteins have important roles in integrating developmental changes of plant in response to biotic stress (Cabrera *et al.*, 2014). Thus, the understanding of CsLOB1 function in citrus development might be the key to determine its role in pustule formation during Xcc infection. To dissect functions of CsLOB1 in citrus development, we constructed transgenic citrus plants overexpressing or silencing *CsLOB1* by using the canker-disease-susceptible 'wanjincheng' orange.

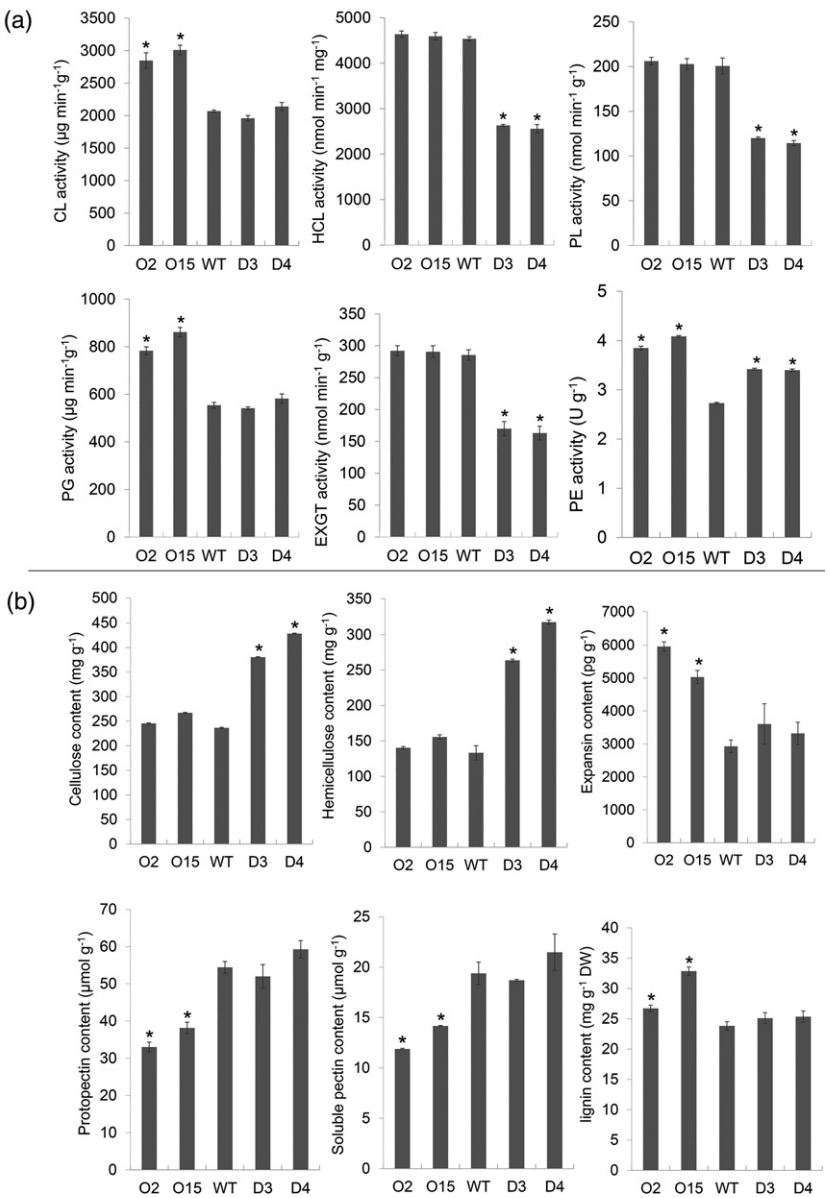

Figure 5. CsLOB1 positively regulated cell wall degradation and modification.
(a) Activity analysis of cell wall degradation and modification-related enzymes in transgenic plants. Hemicellulases (HCL), polygalacturonases (PG), pectin esterases (PE), pectate lyases (PL) and endoxyloglucan transferases (EXGT) were determined in fully mature leaf of transgenic lines. Their activities were calculated using fresh leaf weight as internal reference.
(b) Quantitative analysis of the main components of cell walls in transgenic plants. Protopectin, soluble pectin, hemicellulose, cellulose, expansin proteins and lignin were extracted from fully mature leaf. Their contents were calculated using dry leaf weight as internal reference excepted for expansin proteins, which uses fresh leaf weight as reference. Values are expressed as means ± standard deviation of three independent replicates. *on top of the bars represents significant differences from WT controls based on Duncan's test ($P < 0.01$). O2 and O15, *CsLOB1*-overexpressing transgenic lines; WT, wild-type; D3 and D4, *CsLOB1*-silenced transgenic lines.

CsLOB1 overexpression induced adventitious buds from the axillary bud of transgenic plants, indicating that CsLOB1 play a positive role in lateral organ development in citrus. During 4 years of observation of our transgenic plants, we verified that overexpression of *CsLOB1* can elicit a process of pustule- and canker-like development, confirming that CsLOB1 alone triggers pustule formation and can induce canker-like symptoms. Further, it has been reported that pustules induced by Xcc display hypertrophy and hyperplasia in the plant tissue (Swarup *et al.*, 1991; Duan *et al.*, 1999), which are caused by cell enlargement and proliferation, respectively. In our experiments, no obvious hypertrophy was detected in transgenic plants. However, microscopic analysis showed that pustule-like bulge formation induced by overexpression of *CsLOB1* was due to over-proliferation of cells. This over-proliferation is fully similar to hyperplasia induced by Xcc infection (Swarup *et al.*, 1991), and by transient expression of the Xcc effector gene *pthA4* in *C. sinensis* leaf (Duan *et al.*, 1999). Moreover, we found that the layer number of spongy mesophyll cells was markedly increased by overexpression of *CsLOB1*. It is well known that Xcc invades leaf tissues mostly through stomata and grows in the abundant intercellular space of the spongy mesophyll (Duan *et al.*, 1999; Graham *et al.*, 2004), indicating that CsLOB1 specifically remodels the spongy mesophyll environment to favor pathogen feeding and growth. For example, increasing spongy cells and leaf tissue provides more intercellular

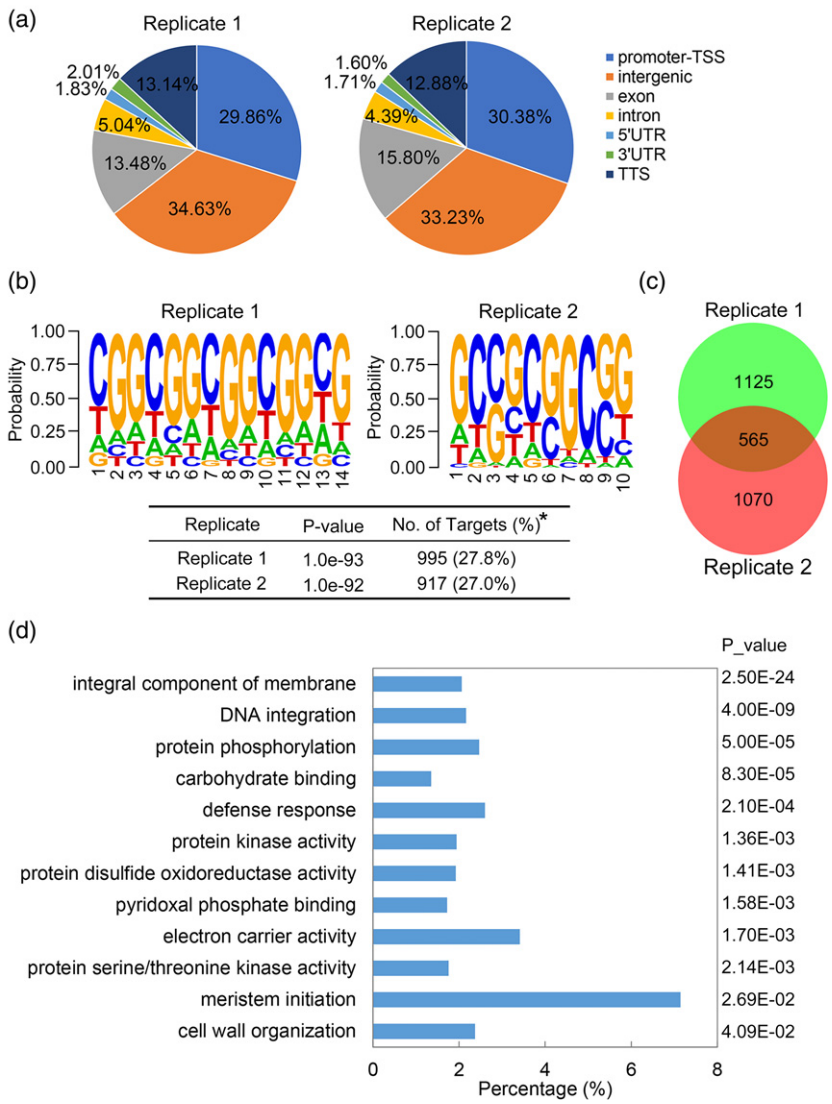

Replicate	P-value	No. of Targets (%)*
Replicate 1	1.0e-93	995 (27.8%)
Replicate 2	1.0e-92	917 (27.0%)

Figure 6. Genome-wide analysis of CsLOB1-targeted genes.
(a) Genome-wide distribution analysis of CsLOB1-binding peaks in two biological replicates by chromatin immunoprecipitation-sequencing (ChIP-seq). TSS, the nearest transcription start site; UTR, untranslated; TTS, transcription termination site.
(b) Motif of the most highly enriched CsLOB1-binding site identified by HOMER software in two biological replicates. *The percentage of targeted sequences covered by motif out of the total number of targeted sequences. The *P*-value of one-tailed binomial test is also shown.
(c) Venn diagram analysis of putative CsLOB1-targeted genes between the two biological replicates.
(d) Gene ontology (GO) enrichment analysis of the 565 identified CsLOB1-targeted genes shared by two biological replicates. Twelve representative overrepresented GO terms and the corresponding *P*-values are shown. The percentage is the ratio of genes annotated to a GO term in the 565 CsLOB1-targeted genes using all unigenes from the *Citrus sinensis* genome database (Xu *et al.*, 2013) as reference.

spaces and nutrition for the pathogen. Though *CsLOB1* overexpression did not affect the entry of Xcc into the leaf tissues, we verified that CsLOB1 can play a role in stomatal structure development. Additionally, RNA-seq and ChIP-seq analyses showed that several cell division and development-related genes were upregulated or targeted by CsLOB1. As shown by infection tests, CsLOB1-induced hyperplasia phenotype significantly enhanced plant susceptibility to Xcc. Based on these data, we conclude that CsLOB1 activates cell proliferation in citrus, and this mechanism can favor pustule and symptom development during Xcc infection.

Finally, cell death and necrosis symptoms, which appear at the later stage of citrus canker disease, are important for bacterial spread on the surface of plants and among individual plants in fields (Duan *et al.*, 1999). The ability to rupture the citrus epidermis is a major factor in both the severity of citrus canker and in its epidemiology (Brunings and Gabriel, 2003). Interestingly, some canker-like bulges in *CsLOB1*-overexpressing plants showed brown corky volcano-like symptoms and cell death, which are similar to pathogen-elicited epidermis rupture, suggesting CsLOB1 also contributes to necrosis at the later stage of infection.

CsLOB1 promotes cell proliferation possibly through mediation of phytohormone signaling

The roles of LBD proteins in phytohormone signaling have also been demonstrated in some crops (Xu *et al.*, 2016). LBD proteins regulate lateral organ initiation and patterning as well as root development via mediating auxin distribution and signaling (Bureau and Simon, 2008; Bureau *et al.*, 2010). However, our RNA-seq data showed that no genes that mediate auxin distribution (such as *PIN*s gene; Bureau and Simon, 2008) were affected by *CsLOB1* overexpression.

Table 1 Functional annotation of CsLOB1-targeted genes based on intersection of ChIP-seq and RNA-seq data

Gene ID	Putative function	Log_2 (fold change) (transgenic line/WT)	
		O2 line	O15 line
		O2 line	
Cell wall			
Cs2g19350	Fasciclin-like arabinogalactan-protein 2 involved in cell wall organisation	1.80	2.52
Cs4g08750	Fasciclin-like arabinogalactan-protein 1 involved in cell wall organisation	3.19	4.55
Cs2g20750	Cellulases and β-1,4-glucanases involved in cell wall degradation	3.74	4.57
orange1.1t02719	Pectin esterases (PME) involved in cell wall modification	1.86	3.46
Hormone metabolism			
Cs9g14190	EXORDIUM-like 3 involved in brassinosteroid signal transduction	2.60	3.45
orange1.1t05518	UDP-glucosyl transferase (UGT85A2) involved in cytokinin metabolism	6.03	5.84
Transcription factor			
Cs4g02590	Transcriptional factor (bHLH family) involved in cell and organ elongation development via brassinosteroid and gibberellin signaling	4.05	4.13
Cs9g03820	Ethylene-responsive transcription factor RAP2-3	−1.09	−0.79
Secondary metabolism			
Cs3g07770	Arogenate dehydratase involved in phenylalanine biosynthesis	0.91	1.97
Transporter			
Cs5g25370	Ammonium transporter 1;4 (AMT1;4)	−2.41	−2.19

Exogenous application of NAA strongly induced *CsLOB1* expression, suggesting *CsLOB1* responses to auxin induction. Likewise, it was further shown that exogenous application of auxin can enhance pustule formation and canker development in citrus (Cernadas and Benedetti, 2009). Interestingly, it was reported that Xcc can produce indole-3-acetic acid (the major form of auxin in plants), and its biosynthesis is increased in the presence of citrus leaf extracts (Costacurta *et al.*, 1998). Indeed, auxin inhibits the translocation of CsMAF1, a repressor of citrus RNA polymerase (Pol) III, from the nucleoplasm to nucleolus and thus releases Pol III to activate the transcription of host genes, which facilitates cell division and growth (Soprano *et al.*, 2017; Oliveira Andrade *et al.*, 2020). CsMAF1 also was shown to bind the PthA4 effector physically (Soprano *et al.*, 2013; Oliveira Andrade *et al.*, 2020). Thus, it is possible that auxin promotes *CsLOB1* expression by enhancement of Pol III and PthA4 functions during Xcc infection (Zou *et al.*, 2019). *CsLOB1* overexpression in transgenic lines might bypass the *CsLOB1*-dependent induction by auxin and thereby promote citrus canker symptoms.

Cytokinins control aspects of almost all plant growth and development processes, including cell division, nutrient allocation and photosynthetic performance (Emery and Kisiala, 2020). Here, we showed that *CsLOB1* overexpression caused dwarfism phenotypes, including the loss of apical dominance and increased branching development, which are similar to phenotypes observed in transgenic apple, Arabidopsis and Populus overexpressing *MdLBD11* (Wang *et al.*, 2013), *LOB*/*MDC12.5* (Shuai *et al.*, 2002) and *PtaLBD1* (Yordanov *et al.*, 2010), respectively. Our previous studies demonstrated that disruption of CK homeostasis resulted in similar phenotypes, including thicker leaves, adventitious branches and the loss of apical dominance in citrus (Zou *et al.*, 2013; Peng *et al.*, 2015). RNA-seq analysis showed that *CsLOB1* overexpression significantly upregulated the 'cytokinins synthesis-degradation' pathway, and remarkedly induced expression of three UGT85A2 genes. UGT85A2-mediated deactivation of CK is a key regulator responsible for maintaining CK homeostasis in plants (Šmehilová *et al.*, 2016). ChIP-seq experiments further identified one *UGT85A2* DEG (orange1.1t05518) as directly targeted by CsLOB1, indicating CsLOB1 directly modulated CK homeostasis. Remarkably, there are reports showing the inhibitory effect of CK on lateral root formation (Li *et al.*, 2006; Laplaze *et al.*, 2007). These data suggest that CsLOB1 promotes cell division and growth through UGT-mediated deactivation of CK.

Moreover, overexpression of *CsLOB1* downregulated the BRS (Cs7g11940) and DWF5 (novel.791) genes (Data S4), whose homologs are involved in BR deactivation and dwarfism phenotypes in other crops (Nolan *et al.*, 2020). Importantly, our RNA-seq and ChIP-seq data indicated that *CsLOB1* directly bind the promoter of *EXO* (Cs9g14190) and activate its expression (Figure S15; Table 1). EXO mediates BR signaling transduction and contributes to cell expansin in Arabidopsis leaves (Schröder *et al.*, 2009). BR hormone was shown to promote stem elongation and cell proliferation (Bell *et al.*, 2012), thus it is reasonable to assume that *CsLOB1* contributes to cell division and growth through the BR signaling pathway.

Finally, two DEGs involved in the ABA signal pathway were upregulated by *CsLOB1*, while all the DEGs in the JA

and salicylic acid (SA) signal pathways were downregulated by *CsLOB1*. However, these DEGs were not detected in our ChIP-seq analysis, which indicates that the expression of these genes might be indirectly activated by CsLOB1. JA regulates plant development in many aspects, including inhibition of seed germination, promoting lateral root formation and inducing root regeneration (Huang *et al.*, 2017). Interestingly, our group previously showed that ABA cooperated with JA and SA signaling to affect Xcc-induced pustule formation and the susceptibility to citrus canker in sweet orange (Long *et al.*, 2019). Together, these data above strongly indicate that CsLOB1 regulates cell division and growth via mediation of hormone signaling. Future studies involving metabolomic analysis to determine CK and BR concentrations in *CsLOB1*-overexpressing and -silenced lines as well as WT plants will be interesting to verify if *CsLOB1* expression can indeed modulate their synthesis and accumulation.

CsLOB1 triggers cell proliferation and contributes to pathogen infection via activation of plant cell wall degradation

The cell wall participates in cell expansin and growth, and provides mechanical support and strength for the plant; meanwhile, the cell wall is a key site attacked and fed by pathogens because it is the first barrier for bacterial infection and a storage for carbohydrates and other molecules (Bellincampi *et al.*, 2014). Thus, microbial phytopathogens must degrade the host cell wall to successfully invade and feed plant tissue. It is well known that many phytopathogens secrete plant cell wall-degrading enzymes such as CL, pectinases, xylanases or endoglucanases to rupture the plant cell wall in the initial stage of infection (Lionetti *et al.*, 2012; Rui *et al.*, 2017).

On the other hand, phytopathogens can further induce host gene expression to degrade the plant cell wall during the infection process. Xcc strongly increases transcription of host genes encoding both enzymes involved in cell wall remodeling and factors associated with cell division and expansin (Cernadas *et al.*, 2008). Indeed, expression of *CsLOB1* is associated with expression of numerous cell wall-related genes (Hu *et al.*, 2014; Duan *et al.*, 2018). Here, our data further confirmed that *CsLOB1* overexpression increased not only transcripts of genes encoding cell wall-degrading and -modifying enzymes, but also the enzymatic activities of their products in these transgenic lines. Because the cell wall main components fall into three broad classes: cellulose, hemicellulose and pectin, we found pectin was decreased by *CsLOB1* overexpression whist cellulose and hemicellulose were increased by *CsLOB1* silence. The increase of cellulose and hemicellulose contents in *CsLOB1*-silenced plants may improve defense against pathogen infection. Likewise, we found *CsLOB1* overexpression increased PG activities, and decreased both protopectin and soluble pectin contents. Pectin is a critical building block in the cell walls of plants, and plays an important role in cell wall stiffness as well as susceptibility to pathogens (Cosgrove, 2015; Zhang and Zhang, 2020). Plant cell wall disruption and expansin require pectin degradation by endogenous pectinases such as PGs and PLs (Rui *et al.*, 2017; Uluisik and Seymour, 2020). Thus, CsLOB1 can activate pectin depolymerization by controlling PG genes expression. Several PE genes were significantly activated by *CsLOB1* overexpression in our transcriptome data. PE-induced pectin methylesterification and demethylesterification were shown to affect cell wall mechanical properties (Cosgrove, 2015); for example, the tissue elasticity in Arabidopsis primordia is correlated with pectin demethylesterification (Peaucelle *et al.*, 2011). Finally, intersection analysis of ChIP-seq and RNA-seq data identified cell wall remodeling-related genes encoding fasciclin-like arabinogalactan-proteins, CL and PEs that were both targeted and activated by CsLOB1, suggesting that CsLOB1 directly activated these genes to degrade and modify cell walls. However, no expansin encoding genes directly targeted by CsLOB1 were detected in ChIP-seq assay, whereas CsLOB1 overexpression greatly increased both expansin expression levels and expansin contents. These results indicate that CsLOB1 indirectly upregulates expression of expansin genes by an unknown pathway. Expansin proteins, which are cell wall-loosening proteins, have a broad range of biological roles in plant growth and development, and response to abiotic and biotic stresses (Choi *et al.*, 2006). In accordance with the presented data, we believe that CsLOB1 promotes cell wall degradation through activation of pectin degradation or modification and accumulation of expansin proteins, which facilitate host cell proliferation as well as pathogen infection and spreading in infected sites.

CsLOB1-targeted genes are involved in cell wall remodeling and hormone signaling

The understanding about downstream mechanisms regulated by the susceptibility gene *CsLOB1* is elusive in the literature. Here, 10 CsLOB1-targeted genes were identified by the analysis of ChIP-seq coupled with RNA-seq data. Among them, four genes encode important enzymes or proteins involved in cell wall organization, degradation and modification, which indicates that CsLOB1 can rapidly promote cell wall remodeling in response to pathogen infection. Two genes are involved in CK and BR hormone pathways (Table 1). Recently, Duan *et al.* (2018) reported that CsLOB1 can interact with the promoter of a zinc finger encoding gene (Cs2g20600) from *C. paradisi* via bioinformatic analysis and electrophoretic mobility shift assays. Likewise, our RNA-seq analysis showed that another zinc finger gene (Cs1g23230) was differentially expressed in *C. sinensis CsLOB1*-overexpressing lines (log2fold change > 3.7; Data S4). However, it was not identified as a

CsLOB1-targeted gene in the ChIP-seq assay. However, our RNA-seq and ChIP-seq data displayed many transcription factor genes that were affected or targeted by CsLOB1 (Data S4 and S7) and, among them, the *IBH1-like 1* (Cs4g02590) was shown to be both targeted and upregulated by CsLOB1 (Table 1). This gene belongs to the basic helix-loop-helix (bHLH) transcriptional regulator family, and can act as a positive or negative regulator by affecting gene expression in response to different signals (Pires and Dolan, 2010; Goossens *et al.*, 2017). The IBH1 acts by forming a heterodimer with another transcription factor BHLH49, and inhibiting the latter to bind to DNA (Zhang *et al.*, 2009). These data imply that CsLOB1 regulates plant development and defense response by a hierarchical transcriptional cascade manner. In rice and Arabidopsis, IBH1 homolog hinders cell and organ elongation in response to BR and GA signaling (Bai *et al.*, 2012). However, no GA-related genes were affected by CsLOB1 in the RNA-seq test, suggesting CsLOB1 acts BR signaling by targeting *IBH1-like 1*. Interestingly, overexpression of *IBH1* homolog causes plant dwarfing (Ikeda *et al.*, 2012). On the other hand, two bHLH (bHLH3 and bHLH6) homologs were identified as susceptibility genes, and directly targeted and activated by the *X. gardneri* TAL effector AvrHah1 (Schwartz *et al.*, 2017). Upregulation of both bHLH3/bHLH6 transcriptional factors induced the expression of a PL, which is involved in maceration of plant tissue to promote water-soaked symptoms on tomato leaves during bacterial spot disease (Schwartz *et al.*, 2017). Further studies are necessary to determine the function and target genes of *IBH1-like 1* homolog in citrus. In addition, a 6-bp LBD motif (GCGGCG), which was previously reported to physically interact with LOB domain proteins (Husbands *et al.*, 2007), was mapped in the promoter regions of enriched genes revealed by our ChIP-seq data. Overall, our data suggest that CsLOB1-targeted genes are mainly involved in cell wall remodeling, CK metabolism and BR signaling. Future investigations will be important to confirm and characterize the interactions of these targeted genes and CsLOB1.

A model of CsLOB1-mediated regulatory mechanism of citrus canker disease

In this study, we demonstrated that CsLOB1 as a major regulator orchestrates a complex regulation network in response to citrus canker pathogen attack. Based on our findings, a model was proposed to explain how Xcc bacteria hijack CsLOB1 functions in plant development to establish pathogen feeding site, colonization and spreading in citrus leaf mesophyll (Figure 7). According to this model, Xcc-induced *CsLOB1* expression promotes host cell proliferation in infected tissue through hormone signaling and cell wall degradation and modification pathways, which contributes to citrus canker development and bacteria growth. Overall, our study provides insight into the regulation mechanism of CsLOB1 in controlling citrus development and pathogen infection, and also offers potential pathways and targeted genes for the biotechnological improvement of citrus canker resistance.

EXPERIMENTAL PROCEDURES

Plant material and bacterial strains

For citrus transformation, 'wanjincheng' orange (*C. sinensis* Osbeck) plants were grown in an orchard of the National Citrus Germplasm Repository, Chongqing, China. All transgenic and WT plants were cultured in a greenhouse maintained at 28°C. The Xcc strain was isolated from naturally infected sweet orange leaves from an orchard in Yunnan province, China. Preparation of the bacterial suspensions for infection experiments was performed as described by Zou *et al.* (2014).

Plant hormone and wounding treatments

The plant hormone treatments were performed as described previously (Long *et al.*, 2019). Fully mature leaves were inoculated with sterile cotton pre-soaked with 5 ml solution of 10 μM NAA, 1 μM ZT, 1 μM BL, 400 μM GA or 100 μM ABA (Sigma, USA), or water. The wounding treatment was carried out as described by Zou *et al.* (2014). The treated samples were cultured in an incubator at 28 , under a 16-h light/8-h dark photoperiod with 60% relative humidity. Induced expressions of *CsLOB1* were analyzed by RT-qPCR. This experiment was repeated three times.

Plasmid construction and citrus transformation

The primers used for vector construction are listed in Table S6. Based on the sequence of the *CsLOB1* (Cs7g27640) gene in the *C. sinensis* genome database (http://citrus.hzau.edu.cn/orange/), the *CsLOB1* coding sequence was amplified from 'wanjincheng' orange by PCR and cloned into the plant expression vector pGN (Peng *et al.*, 2017). Both Cs*LOB1* and *flag:CsLOB1* (FLAG:CsLOB1, which contains FLAG-tag peptide at its N-terminus: DYKDDDDK-DYKDDDDK) were inserted separately downstream of a *CaMV 35S* promoter to generate the overexpression constructs *pOLOB1* and *pflag:LOB*, respectively.

To construct the *CsLOB1* RNAi vector, a 172-bp fragment at the 3′-end of its coding sequence was amplified and cloned as an inverted repeat between the intron from the *Petunia hybrida* Chalcone synthase A gene in the RNAi vector pFGC5941 (GenBank accession nos. AY310901). Finally, this *CsLOB1* RNAi construct was transferred into pGN plasmid and inserted downstream of *CaMV 35S* promoter to generate the RNAi construct *pDLOB1*, which was used to transform 'wanjincheng' orange.

To examine the expression pattern, the promoter of *CsLOB1* from 'wanjincheng' orange (Peng *et al.*, 2017) was fused with the GUS gene in pBI121 vector. The promoter was 497 bp long, which was just upstream to the first codon 'ATG', and included its 5′-untranslated region sequence (Peng *et al.*, 2017).

All the constructed plasmids were verified by sequencing, and introduced into *Agrobacterium tumefaciens* EHA105 for citrus transformation. The transgenic plants were generated from 'wanjincheng' orange epicotyl explants by the *A. tumefaciens*-mediated transformation, as described (Peng *et al.*, 2015). Transgenic plants were selected by GUS histochemical staining and/or PCR amplification. All transgenic and WT control plants were grafted onto *Citrus junos* Sieb. ex *Tanaka* rootstock in a greenhouse. Up- and down-expression of *CsLOB1* in

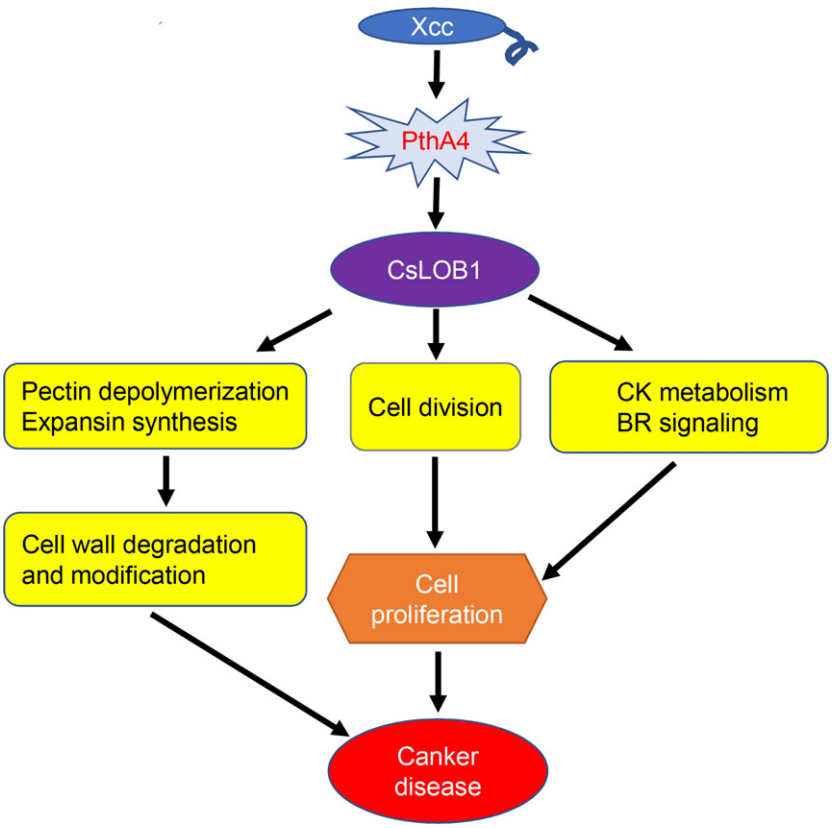

Figure 7. Proposed model of action of CsLOB1 in regulating susceptibility to citrus canker disease. *CsLOB1* expression is induced by the PthA4 effector that is translocated to the host cell by *Xanthomonas citri* subsp. *citri* (Xcc). In turn, CsLOB1 targets downstream host genes involved in pectin depolymerization, accumulation of expansins, cell division, and CK and BR hormone signaling pathways. Depolymerization of pectin and increase of expansin proteins result in cell wall modification, loosing and degradation, which together with activation of cell division factors and CK and BR hormone pathways enhance host cell proliferation and facilitate pathogen feeding and growth at infected sites. Activation of CsLOB1-targeted genes leads to the host cell over-proliferation and thereby favors pustule formation. Overall, host cell changes triggered by induction of CsLOB1 promote citrus canker development. CK, cytokinin; BR, brassinosteroid.

overexpressing and RNAi-silencing *CsLOB1* transgenic plants were confirmed by RT-qPCR. Transgenic plants expressing FLAG-CsLOB1 construct were also confirmed by immunoblot with anti-FLAG antibodies (Abcam ab1162).

Microscopic observations

Wild-type and transgenic tissues were prepared for light microscopic observations. Sample preparation of resin-embedded sections was done as described (Kim *et al.*, 2009). Cross-slides were made on Feica microtome (HEAD Biotechnology, Beijing, China). The samples were stained with 0.01% (g L^{-1}) aniline blue.

Fully mature leaves from 4-year-old plants of various genotypes were used for stomata analysis. Rectangular (about 0.5 cm × 1 cm) leaf tissues were floated on stomatal opening buffer (10 mM MES, pH 6.15 and 30 mM KCl) under light for 3 h to fully open the stomata, and then transferred into 3 mol L^{-1} NaOH solution and were incubated for 15 min at 28°C. The treated tissues were cleaned with ddH_2O, and the lower epidermis were isolated from the tissues and stained with 0.01% (g L^{-1}) aniline blue.

All the samples were imaged by BX51 microscope system equipped with a DP70 digital camera (Olympus, Tokyo, Japan). Leaf thickness and layers, stomatal aperture, and cell size were determined using ImageJ software.

Assays of susceptibility to *Xanthomonas citri* subsp. *citri* in citrus

Assays of susceptibility to Xcc in transgenic plants were performed using *in vitro* pinprick inoculation and *in vivo* infiltration, as described by Peng *et al.* (2017). Fully mature healthy leaves of transgenic and WT plants were infected with 1×10^8 CFU ml^{-1} Xcc. At 9 dpi, citrus canker development was recorded by photographing, and diseased areas and disease severity of leaves of transgenic plants were determined using ImageJ software based on the diseased index reported by Peng *et al.* (2017).

Bacterial growth assays were performed as described by Peng *et al.* (2015), and had minor modification. Briefly, punctures were made in fully mature leaves with a needle, then 1 μl Xcc suspension (1×10^8 CFU ml^{-1}) was dropped onto each pinprick. Three infected pinpricks per transgenic line including WT plants were collected and pooled at 0–9 dpi. The mixed sample is a technical repeat for every line. Three technical repeats were performed per test. Bacterial growth was measured by direct counting of colony-forming units. Bacterial growth was expressed using the number of bacterial cells per pinprick (CFU $pinprick^{-1}$).

Stomata-mediated susceptibility was further evaluated by the spray inoculation (Yang *et al.*, 2011). Ten fully expanded young leaves per line were individually spray-inoculated with 1×10^8 CFU ml^{-1} Xcc and incubated in a growth chamber at 28°C, under a 16-h photoperiod. Disease severity was assessed at 30 dpi. The frequencies of diseased leaf were numbered. The images of inoculated leaves were digitalized, and total and diseased leaf areas were calculated by ImageJ software. The disease severity was calculated by dividing the total diseased area with the total area of inoculated leaves and expressed as a percentage.

For pathogen entry assays (Su *et al.*, 2017), fully expanded young leaves were first treated with 45 μmol m^{-2} sec^{-1} illumination for 2.5 h to fully open stomata, and then treated with 1×10^8 CFU ml^{-1} Xcc for 1 h. The treated leaves were washed with 0.02% Silwet L-77 three times, and then with sterilized water

three times. Pathogen entry was measured by direct counting of colony-forming units.

All the above tests were repeated three times.

RNA-seq and analysis

For transcriptome analysis, three biological replicates per selected transgenic and WT plants were performed. Total RNAs from fully mature leaves were used to construct sequencing libraries. RNA preparation and sequencing library construction were performed as described by Zou *et al.* (2019). The libraries were sequenced with the Illumina Hiseq 2500 platform (Novogene, Beijing, China). Adaptor, rRNA and tRNA sequences were filtered from raw reads using Bowtie2 (Langmead and Salzberg, 2012) and, then, all the clean reads were mapped to sweet orange genome (http://citrus.hzau.edu.cn/orange/index.php) by HISAT 2.0.5 software (Kim *et al.*, 2015a). Quantification of read counts per gene in all biological replicates was estimated by featureCounts (Liao *et al.*, 2014). Using WT as control, DEGs in transgenic plants were screened according to the following thresholds of |fold change| ≥ 1.5, and adjusted *P*-value < 0.05 using the DESeq2 package (Love *et al.*, 2014). Gene functions were also annotated based on Nr, Nt, Pfam, KOG/COG, Swiss-Prot, KO and GO databases.

MapMan software (Thimm *et al.*, 2010) was used to visualize the RNA-seq data as described previously (Zou *et al.*, 2019). MapMan uses a plant-specific ontology that classifies genes into well-defined hierarchical pathway or function categories, denominated BINs. Briefly, all genes from the RNA-seq data were firstly assigned to BINs using the Mercator automated annotation pipeline (http://mapman.gabipd.org/web/guest/mercator) to construct a MapMan BINs annotation file and, then, all the DEGs from every transgenic line were mapped to the file to visualize MapMan pathways or functions. Differentially represented MapMan pathways or functions were defined by a two-tailed Wilcoxon rank sum test corrected by the Benjamin–Hochberg method (FDR ≤ 0.05).

ChIP-seq and analysis

The ChIP-seq assays were performed according to the method previously described by Li *et al.* (2017). Briefly, 1 g transgenic citrus leaves with *flag:CsLOB1* was harvested and cross-linked with 1% (v/v) formaldehyde for 10 min, and quenched by addition of 125 mmol L^{-1} glycine. Subsequently, the chromatins were isolated, sonicated and immunoprecipitated with polyclonal anti-FLAG antibodies (Abcam ab1162). The ChIP DNA and input DNA were recovered and dissolved in water for ChIP-seq. Immunoprecipitated DNA was used to construct sequencing libraries following the protocol provided by the I NEXTFLEX® ChIP-Seq Library Prep Kit for Illumina® Sequencing (NOVA-514120; Bioo Scientific, Beijing, China), and then sequenced on Illumina Hiseq 2500 platform (Novogene) with PE 150 method. Clean reads were mapped to the sweet orange genome by Bwa (version 0.7.15; Li and Richard, 2010). Samtools (version 1.3.1) was used to remove potential PCR duplicates (Li *et al.*, 2010). MACS2 software (version 2.1.1.20160309) was used to call peaks by default parameters (bandwidth, 300 bp; model fold, 5, 50; *q*-value, 0.05). If the summit of a peak is located closest to the TSS (the nearest transcription start site) of one gene, the peak will be assigned to that gene (Salmon-Divon *et al.*, 2010). HOMER (version3) was used to predict motif occurrence within peaks with default settings for a maximum motif length of 14 base pairs (Hull *et al.*, 2013). Overlapping peaks between biological replicates were retrieved using the R package BEDTools with default parameters (Patwardhan *et al.*, 2019). GO enrichment analysis of the CslOB1-targeted genes was conducted in the Biocloud website (BioMarker Technologies Illumina, Shanghai, China) using all unigenes from the *C. sinensis* genome database (Xu *et al.*, 2013) as background reference. Differentially represented GO terms were screened based on *P*-values ($P < 0.05$).

Measurement of cell wall components

Full mature leaf was used to investigate cell wall-related components in transgenic plants. Isolation and activity detection of CL, HCL, PG, PE, PL and EXGT enzymes were performed according to the protocols of the corresponding enzyme activity detection kits (Sino Best Biological Technology, Shanghai, China). Isolation and content determination of protopectin, soluble pectin, hemicellulose, cellulose and lignin were also carried out according to the protocols of the corresponding quantitative kits (Sino Best Biological Technology). Expansin protein extraction and its content measurement were determined using the plant expansin ELISA kits (Sino Best Biological Technology).

RT-qPCR analysis

The primers used for this experiment are listed in Table S6. Citrus total RNA was isolated using the EASYspin Plant RNA Extraction Kit following the manufacturer's instructions (Aidlab, Beijing, China). RNA was reverse transcribed into cDNA using the iScriptTM cDNA Synthesis Kit (Bio-Rad, Hercules, CA, USA). The detection of gene expression was performed by PCR using the iQ™ SYBR Green Supermix (Bio-Rad), as previously described (Zou *et al.*, 2019). The relative expression levels were calculated by the $2^{-\Delta\Delta Ct}$ method (Livak and Schmittgen, 2002), and the citrus actin gene (Zou *et al.*, 2019) was used for normalization.

ACKNOWLEDGEMENTS

This work was supported by the National Key Research and Development Program of China (2018YFD1000300, to SC), the National Natural Sciences Foundation of China (31972393, to XZ), and the Earmarked Fund for China Agriculture Research System (CARS-27, to SC). M.A. was supported by Fundação de Amparo à Pesquisa do Estado de São Paulo (FAPESP) post-doctoral scholarship (2017/18570-9).

CONFLICT OF INTEREST

The authors declare that they have no conflict of interest.

AUTHOR CONTRIBUTIONS

XZ designed the experiments, analyzed the data and wrote the manuscript. MD performed the RNA-seq experiment. YL performed analysis of the promoter, and PCR and RT-qPCR. LW performed microscopic observation and disease susceptibility analysis. LX performed citrus transformation. QL performed cell wall-related enzymatic activity and components analysis. AP and YH performed ChIP-seq experiment. MA critically revised the manuscript, and S.C. analyzed the data. All of the authors read and approved the manuscript.

DATA AVAILABILITY STATEMENT

RNA-seq and ChIP-seq raw data were deposited at GenBank under BioProject identifier PRJNA670516.

SUPPORTING INFORMATION

Additional Supporting Information may be found in the online version of this article.

Figure S1. *CsLOB1* expression analysis in the presence of ZT, BL, GA or ABA hormones in 'wanjincheng' orange leaf. *CsLOB1* expressions in treated leaf were determined by RT-qPCR. Relative expression levels were calculated by comparing with mock control. Values are expressed as means ± standard deviation of three independent tests. No significantly induced expression was detected at 12, 24, 36 and 48 h after hormone treatment compared with that at 0 h (a Duncan's test, $P < 0.05$). ZT, zeatin; BL, brassinolide; GA, gibberellin; ABA, abscisic acid.

Figure S2. Relative expression analysis of *CsLOB1* transgenic plants. (a) T-DNA structure of the *pOLOB1* and *pDLOB1* vectors. *CaMV 35S*, tobacco *Cauliflower mosaic virus 35S* promoter; *GUS:NPTII*, fusion of β-glucuronidase and neomycin phosphotransferase genes; *nos*, nos terminator; *LB*, left border; *RB*, right border; CHSA intron, the intron from the *Petunia hybrida* Chalcone synthase A gene. (b) and (c) Compared with WT control plants, the relative expression of *CsLOB1* in transgenic plants was determined by RT-qPCR. Citrus actin gene was used as reference. Total RNAs were extracted from three fully mature leaves per line. For WT control, three fully mature leaves were harvested from three plants. Values are expressed as means ± standard deviation of three independent tests. Relative folds were shown by Log2 (relative expression). WT, wild type; O#, *CsLOB1*-overexpressing transgenic lines; D#, *CsLOB1*-silenced transgenic lines. The data showed that seven out of 11 *CsLOB1*-overexpressing plants had high levels of gene expression, and eight out of 14 *CsLOB1*-silenced plants had significantly decreased gene expression, compared with WT plants.

Figure S3. Phenotypes of 1-year-old transgenic plants in greenhouse. WT, wild type; O#, *CsLOB1*-overexpressing transgenic lines; D#, *CsLOB1*-silenced transgenic lines.

Figure S4. Phenotypes of 4-year-old transgenic plants in greenhouse. WT, wild type; O#, *CsLOB1*-overexpressing transgenic lines; D#, *CsLOB1*-silenced transgenic lines.

Figure S5. Leaf shapes of transgenic plants growing in a greenhouse. (a) The representative leaves of transgenic and WT plants. The longitudinal (b), transverse (c) diameters, leaf shape index (length/width) (d) and leaf area (e) of 4-year-old transgenic plants were evaluated using 20 leaves per line. Values are expressed as means ± standard deviation of three independent tests. Different letters on top of the bars represent significant differences from WT controls based on Duncan's test ($P < 0.05$). WT, wild type; O#, *CsLOB1*-overexpressing transgenic lines; D#, *CsLOB1*-silenced transgenic lines.

Figure S6. Development of adventitious buds (red arrowheads) and pustule- and canker-like bulges (red arrows) in 4-year-old transgenic plants overexpressing *CsLOB1* in greenhouse. WT, wild type; O#, *CsLOB1*-overexpressing transgenic lines.

Figure S7. Pustule- and canker-like bulges in leaves from 4-year-old transgenic plants overexpressing *CsLOB1* in greenhouse. WT, wild-type.

Figure S8. Pustule- and canker-like bulges in stems from 4-year-old transgenic plants overexpressing *CsLOB1* in greenhouse. WT, wild-type; O#, *CsLOB1*-overexpressing transgenic lines.

Figure S9. Relative expression of *CsLOB1* in different tissues from O2 and O15 transgenic lines. Gene expressions in bulge-like and normal tissues of leaf, adventitious and normal buds from O2 and O15 transgenic lines were investigated by RT-qPCR using WT tissues as control. The data showed that *CsLOB1* expression levels in bulge-like tissues (a) and in adventitious buds (b) were obviously higher than these in normal tissues and buds, respectively. Actin gene was used as an internal control. Values are expressed as means ± standard deviation of three independent tests. *Represents significant differences from WT controls based on Duncan's test ($P < 0.05$). WT, wild type; O#, *CsLOB1*-overexpressing transgenic lines.

Figure S10. Evaluation of susceptibility to *Xanthomonas citri* subsp. *citri* (Xcc) in transgenic plants. Fully mature healthy leaves of transgenic and WT plants were infected with 1×10^8 CFU ml^{-1} Xcc. Leaf disease areas (mm^2) caused by Xcc infection were determined at 9 days post-inoculation (dpi). Values are expressed as means ± standard deviation of three independent tests. Different letters on top of the bars represent significant differences from WT controls based on Duncan's test ($P < 0.05$). In (a), scale bar: 1 cm. WT, wild type; O#, *CsLOB1*-overexpressing transgenic lines; D#, *CsLOB1*-silenced transgenic lines.

Figure S11. *In vivo* assay of citrus canker susceptibility on transgenic plants. Leaves were infiltrated with *Xanthomonas citri* subsp. *citri* (Xcc) suspensions. Fully mature healthy leaves of transgenic and WT plants were infected with 1×10^8 CFU ml^{-1} Xcc. Photographs were recorded 8 days after infiltration. O2 and O15, *CsLOB1*-overexpressing transgenic lines; WT, wild-type; D3 and D4, *CsLOB1*-silenced transgenic lines.

Figure S12. Expression levels of *CsLOB1* in response to inoculation of *Xanthomonas citri* subsp. *citri* (Xcc) in *CsLOB1*-silenced transgenic lines D3 and D4. Fully mature healthy leaves of transgenic and WT plants were infected with 1×10^8 CFU ml^{-1} Xcc by infiltration. Relative expressions of *CsLOB1* in leaves were determined by RT-qPCR at 1, 3, 5, 7 and 9 dpi (days post-inoculation). Values are expressed as means ± standard deviation of three independent tests. *Represent significant differences from WT controls based on Duncan's test ($P < 0.05$). The data showed that the Xcc-induced expression levels of *CsLOB1* in *CsLOB1*-silenced transgenic lines were remarkedly lower than those of the WT control.

Figure S13. Changes of stomata aperture in leaf of transgenic plants. (a) and (b) Microscopic observation of stomata aperture in fully mature leaf from transgenic plants. The slides were stained with 0.01% (g L^{-1}) aniline blue. White arrowheads indicated the keratinous protuberance outside stomatal guard cell wall; double arrows indicated the size of stomata entry. Scale bar: 50 μm. (c) The opening area and length and width of stomatal aperture were evaluated using 20 slides from six leaves per line. Values are expressed as means ± standard deviation of three independent experiments. '*' on top of the bars represents significant differences from WT controls based on Duncan's test ($P < 0.05$). O2 and O15, *CsLOB1*-overexpressing transgenic lines; WT, wild-type; D3 and D4, *CsLOB1*-silenced transgenic lines.

Figure S14. Overview of RNA-seq data from four transgenic plants. (a) Volcano plot (significance versus fold change) of significantly altered genes (|fold change| ≥ 1.5 and FDR < 0.05) between transgenic and WT plants. (b) Venn diagrams showing the overlaps of DEGs among transgenic lines.

Figure S15. Validation of DEGs by RT-qPCR analysis. Relative expressions of 32 selected DEGs regulated by CsLOB1. The *y*-axis on the left shows corresponding expression data of DEGs (gray histogram), while the *y*-axis on the right shows the relative expressions analyzed by RT-qPCR (black lines). Actin gene was used as an internal control. Values are expressed as means ± standard deviation of three independent tests. O2 and O15, *CsLOB1*-overexpressing transgenic lines; WT, wild-type; D3 and D4, *CsLOB1*-silenced transgenic lines.

Figure S16. Characterization of *flag:CsLOB1* transgenic plants. (a) Expression levels of *flag:CsLOB1* in transgenic plants compared with WT control. Relative expressions of *flag:CsLOB1* in transgenic plants were determined by RT-qPCR, using the citrus actin gene as reference. Values are expressed as means ± standard deviation of three independent experiments. (b) Western blotting analysis of FLAG:CsLOB1 proteins in transgenic plants. Leaf protein was blotted and probed with anti-FLAG tag and β-actin antibodies. β-actin was used as a loading control. The result showed that *flag:CsLOB1-1* and *flag:CsLOB1-2* plant lines had high levels of FLAG:CsLOB1 proteins. Thus, the two plants were used in the ChIP-seq experiment.

Figure S17. Overview of ChIP-seq data from two biological replicates. Number of total reads, mapped reads and unique reads in each data set are shown. R1-ChIP and R2-ChIP, replicate 1 and 2 tests, respectively; R1-Input and R2-Input, replicate 1 and 2 controls, respectively. The value was expressed in exponential notation, replacing part of the number with E + n, where E multiplies the preceding number by 10 to the n*th* power.

Figure S18. The irreproducible discovery rate (IDR) framework for assessing the reproducibility of ChIP-seq data sets. (a) Scatter plots of ranks of peaks that overlap each pair of replicates. Note that low ranks correspond to high signal and vice versa. (b) Scatter plots of signal scores of peaks that overlap two replicates. (c) and (d) The estimated IDR as a function of different rank thresholds.

Figure S19. Distribution of the distance of the center of the peaks to the nearest TSS in the two biological replicates.

Figure S20. Analysis of putative CsLOB1-targeted genes. (a) Intersection analysis of ChIP-seq and RNA-seq data. Through the 565 CsLOB1-targeted genes shared by the two replicates (Replicate1_2) in ChIP-seq results, intersection analysis was performed among ChIP-seq and RNA-seq data of the O2 and O15 lines. (b) Expression analysis of 10 CsLOB1-targeted genes during *Xanthomonas citri* subsp. *citri* infection. Transcript levels in leaves were determined by RT-qPCR at 1, 2, 3 and 5 days post-inoculation (dpi). Values are expressed as means ± standard deviation of three independent tests.

Table S1. Survival rate of transgenic plants via grafting.

Table S2. Stomatal density in transgenic plants.

Table S3. Summary of sequencing data for each sample.

Table S4. Mapping summary of sequencing data for each sample.

Table S5. Statistical analysis of DEGs in transgenic plants.

Table S6. Primers used in this study.

Data S1. Gene expression levels in all biological replicates were estimated by featureCounts.

Data S2. Upregulated DEGs shared by the O2 and O15 lines.

Data S3. MapMan BINs significantly enriched in transgenic plants.

Data S4. Significantly enriched cellular pathways or functions and related DEGs in the O2 and O15 lines.

Data S5. Overlapping peaks shared by replicates 1 and 2.

Data S6. GO enrichment of CsLOB1-targeted genes shared by replicates 1 and 2.

Data S7. CsLOB1-targeted transcription factor genes shared by replicates 1 and 2.

REFERENCES

Bai, M.-Y., Fan, M., Oh, E. & Wang, Z.-Y. (2012) A triple helix-loop-helix/basic helix-loop-helix cascade controls cell elongation downstream of multiple hormonal and environmental signaling pathways in *Arabidopsis*. *The Plant Cell*, **24**, 4917–4929.

Barnes, W.J. & Anderson, C.T. (2018) Release, recycle, rebuild: cell-wall remodeling, autodegradation, and sugar salvage for new wall biosynthesis during plant development. *Molecular Plant*, **11**, 31–46.

Bell, E., Lin, W., Husbands, A., Yu, L., Jaganatha, V., Jablonska, B. *et al.* (2012) *Arabidopsis* lateral organ boundaries negatively regulates brassinosteroid accumulation to limit growth in organ boundaries. *Proceedings of the National Academy of Sciences of the United States of America*, **109**, 21146–21151.

Bellincampi, D., Cervone, F. & Lionetti, V. (2014) Plant cell wall dynamics and wall-related susceptibility in plant–pathogen interactions. *Frontiers in Plant Science*, **5**, 228.

Brunings, A.M. & Gabriel, D.W. (2003) *Xanthomonas citri*: breaking the surface. *Molecular Plant Pathology*, **4**, 141–157.

Bureau, M., Rast, M.I., Illmer, J. & Simon, R. (2010) JAGGED LATERAL ORGAN (JLO) controls auxin dependent patterning during development of the *Arabidopsis* embryo and root. *Plant Molecular Biology*, **74**, 479–491.

Bureau, M. & Simon, R. (2008) JLO regulates embryo patterning and organ initiation by controlling auxin transport. *Plant Signaling & Behavior*, **3**, 145–147.

Cabrera, J., Díaz-Manzano, F.E., Sanchez, M., Rosso, M.-N., Melillo, T., Goh, T. *et al.* (2014) A role for LATERAL ORGAN BOUNDARIES-DOMAIN 16 during the interaction *Arabidopsis-Meloidogyne* spp. provides a molecular link between lateral root and root-knot nematode feeding site development. *New Phytologist*, **203**, 632–645.

Cernadas, A., Camillo, L. & Benedetti, C. (2008) Transcriptional analysis of the sweet orange interaction with the citrus canker pathogens *Xanthomonas axonopodis* pv. *citri* and *Xanthomonas axonopodis* pv. *aurantifolii*. *Molecular Plant Pathology*, **9**, 609–631.

Cernadas, R.A. & Benedetti, C.E. (2009) Role of auxin and gibberellin in citrus canker development and in the transcriptional control of cell-wall remodeling genes modulated by *Xanthomonas axonopodis* pv. *citri*. *Plant Science*, **177**, 190–195.

Choi, D., Cho, H.T. & Lee, Y. (2006) Expansins: expanding importance in plant growth and development. *Physiologia Plantarum*, **126**, 511–518.

Cosgrove, D.J. (2015) Plant cell wall extensibility: connecting plant cell growth with cell wall structure, mechanics, and the action of wall-modifying enzymes. *Journal of Experimental Botany*, **67**, 463–476.

Costacurta, A., Mazzafera, P. & Rosato, Y.B. (1998) Indole-3-acetic acid biosynthesis by *Xanthomonas axonopodis* pv. *citri* is increased in the presence of plant leaf extracts. *FEMS Microbiology Letters*, **159**, 215–220.

Duan, S., Jia, H., Pang, Z., Teper, D., White, F., Jones, J. *et al.* (2018) Functional characterization of the citrus canker susceptibility gene *CsLOB1*. *Molecular Plant Pathology*, **19**, 1908–1916.

Duan, Y.P., Castañeda, A., Zhao, G., Erdos, G. & Gabriel, D.W. (1999) Expression of a single, host-specific, bacterial pathogenicity gene in plant cells elicits division, enlargement, and cell death. *Molecular Plant-Microbe Interactions*, **12**, 556–560.

Emery, R.J.N. & Kisiala, A. (2020) The roles of cytokinins in plants and their response to environmental stimuli. *Plants*, **9**, 1158.

Fan, M., Xu, C., Xu, K. & Hu, Y. (2012) LATERAL ORGAN BOUNDARIES DOMAIN transcription factors direct callus formation in *Arabidopsis* regeneration. *Cell Research*, **22**, 1169–1180.

Ference, C.M., Gochez, A.M., Behlau, F., Wang, N., Graham, J.H. & Jones, J.B. (2018) Recent advances in the understanding of *Xanthomonas citri* ssp. *citri* pathogenesis and citrus canker disease management. *Molecular Plant Pathology*, **19**, 1302–1318.

Fernando Gil, J., Liebe, S., Thiel, H., Lennefors, B.-L., Kraft, T., Gilmer, D. *et al.* (2018) Massive up-regulation of LBD transcription factors and EXPANSINs highlights the regulatory programs of rhizomania disease. *Molecular Plant Pathology*, **19**, 2333–2348.

Goossens, J., Mertens, J. & Goossens, A. (2017) Role and functioning of bHLH transcription factors in jasmonate signalling. *Journal of Experimental Botany*, **68**, 1333–1347.

Graham, J.H., Gottwald, T.R., Cubero, J. & Achor, D.S. (2004) *Xanthomonas axonopodis* pv. *citri*: factors affecting successful eradication of citrus canker. *Molecular Plant Pathology*, **5**, 1–15.

Hu, Y., Zhang, J.L., Jia, H.G., Sosso, D., Li, T., Frommer, W.B. *et al.* (2014) Lateral organ boundaries 1 is a disease susceptibility gene for citrus bacterial canker disease. *Proceedings of the National Academy of Sciences of the United States of America*, **111**, E521–E529.

Huang, H., Liu, B., Liu, L. & Song, S. (2017) Jasmonate action in plant growth and development. *Journal of Experimental Botany*, **68**, 1349–1359.

Hull, R.P., Srivastava, P.K., D'Souza, Z., Atanur, S.S., Mechta-Grigoriou, F., Game, L. *et al.* (2013) Combined ChIP-Seq and transcriptome analysis identifies AP-1/JunD as a primary regulator of oxidative stress and IL-1β synthesis in macrophages. *BMC Genomics*, **14**, 92.

Husbands, A., Bell, E., Shuai, B., Smith, H. & Springer, P. (2007) LATERAL ORGAN BOUNDARIES defines a new family of DNA-binding transcription factors and can interact with specific bHLH proteins. *Nucleic Acids Research*, **35**, 6663–6671.

Ikeda, M., Fujiwara, S., Mitsuda, N. & Ohme-Takagi, M. (2012) A Triantagonistic basic helix-loop-helix system regulates cell elongation in *Arabidopsis*. *The Plant Cell*, **24**, 4483–4497.

Jia, H. & Wang, N. (2020) Generation of homozygous canker-resistant citrus in the T0 generation using CRISPR-SpCas9p. *Plant Biotechnology Journal*, **18**, 1990–1992.

Jia, H., Zhang, Y., Orbović, V., Xu, J., White, F.F., Jones, J.B. *et al.* (2017) Genome editing of the disease susceptibility gene *CsLOB1* in citrus confers resistance to citrus canker. *Plant Biotechnology Journal*, **15**, 817–823.

Kim, D., Langmead, B. & Salzberg, S.L. (2015a) HISAT: a fast spliced aligner with low memory requirements. *Nature Methods*, **12**, 357–360.

Kim, J., Sagaram, U., Burns, J., Li, J. & Wang, N. (2009) Response of sweet orange (*Citrus sinensis*) to '*Candidatus* Liberibacter asiaticus' infection: microscopy and microarray analyses. *Phytopathology*, **99**, 50–57.

Kim, M.-J., Kim, M., Lee, M.R., Park, S.K. & Kim, J. (2015b) LATERAL ORGAN BOUNDARIES DOMAIN (LBD)10 interacts with SIDECAR POLLEN/LBD27 to control pollen development in *Arabidopsis*. *The Plant Journal*, **81**, 794–809.

Langmead, B. & Salzberg, S.L. (2012) Fast gapped-read alignment with Bowtie 2. *Nature Methods*, **9**, 357–359.

Laplaze, L., Benkova, E., Casimiro, I., Maes, L., Vanneste, S., Swarup, R. *et al.* (2007) Cytokinins act directly on lateral root founder cells to inhibit root initiation. *The Plant Cell*, **19**, 3889–3900.

Li, H., Handsaker, B., Wysoker, A., Fennell, T., Ruan, J., Homer, N. *et al.* (2010) 1000 genome project data processing subgroup. The sequence alignment/map (SAM) format and SAMtools. *Bioinformatics*, **25**, 2078–2079.

Li, H. & Richard, D. (2010) Fast and accurate short read alignment with Burrows-Wheeler transform. *Bioinformatics*, **25**, 1754–1760.

Li, N., Wei, S., Chen, J., Yang, F. & Chu, Z. (2017) OsASR2 regulates the expression of a defense-related gene, *Os2H16*, by targeting the GT-1 cis-element. *Plant Biotechnology Journal*, **16**, 771–783.

Li, X., Mo, X., Shou, H. & Wu, P. (2006) Cytokinin-mediated cell cycling arrest of pericycle founder cells in lateral root initiation of *Arabidopsis*. *Plant and Cell Physiology*, **47**, 1112–1123.

Li, Z., Zou, L., Ye, G., Xiong, L., Ji, Z., Zakria, M. *et al.* (2014) A potential disease susceptibility gene *CsLOB* of citrus is targeted by a major virulence effector PthA of *Xanthomonas citri* subsp. *citri*. *Molecular Plant*, **7**, 912–915.

Liao, Y., Smyth, G.K. & Shi, W. (2014) FeatureCounts: an efficient general purpose program for assigning sequence reads to genomic features. *Bioinformatics*, **30**, 923–930.

Lionetti, V., Cervone, F. & Bellincampi, D. (2012) Methyl esterification of pectin plays a role during plant–pathogen interactions and affects plant resistance to diseases. *Journal of Plant Physiology*, **169**, 1623–1630.

Livak, K.J. & Schmittgen, T.D. (2002) Analysis of relative gene expression data using real-time quantitative PCR. *Methods*, **25**, 402–408.

Long, Q., Xie, Y., He, Y., Li, Q., Zou, X. & Chen, S. (2019) Abscisic acid promotes jasmonic acid accumulation and plays a key role in citrus canker development. *Frontiers in Plant Science*, **10**, 1634.

Love, M.I., Huber, W. & Anders, S. (2014) Moderated estimation of fold change and dispersion for RNA-seq data with DESeq2. *Genome Biology*, **15**, 550.

Majer, C. & Hochholdinger, F. (2011) Defining the boundaries: structure and function of LOB domain proteins. *Trends in Plant Science*, **16**, 47–52.

Nolan, T., Vukašinović, N., Liu, D., Russinova, E. & Yin, Y. (2020) Brassinosteroids: multidimensional regulators of plant growth, development, and stress responses. *The Plant Cell*, **32**, 295–318.

Oh, S.A., Park, K.S., Twell, D. & Park, S.K. (2010) The *SIDECAR POLLEN* gene encodes a microspore-specific LOB/AS2 domain protein required for the correct timing and orientation of asymmetric cell division. *The Plant Journal*, **64**, 839–850.

Oliveira Andrade, M., Sforça, M.L., Batista, F.A.H., Figueira, A.C.M. & Benedetti, C.E. (2020) The MAF1 phosphoregulatory region controls MAF1 interaction with the RNA polymerase III C34 subunit and transcriptional repression in plants. *The Plant Cell*, **32**, 3019–3035.

Patwardhan, M., Wenger, C., Davis, E. & Phanstiel, D. (2019) Bedtoolsr: an R package for genomic data analysis and manipulation. *Journal of Open Source Software*, **4**, 1742.

Peaucelle, A., Braybrook, S.A., Le Guillou, L., Bron, E., Kuhlemeier, C. & Höfte, H. (2011) Pectin-induced changes in cell wall mechanics underlie organ initiation in *Arabidopsis*. *Current Biology*, **21**, 1720–1726.

Peng, A.H., Chen, S.C., Lei, T.G., Xu, L.Z., He, Y.R., Wu, L. *et al.* (2017) Engineering canker-resistant plants through CRISPR/Cas9-targeted editing of the susceptibility gene *CsLOB1* promoter in citrus. *Plant Biotechnology Journal*, **15**, 1509–1519.

Peng, A., Xu, L., He, Y., Lei, T., Yao, L., Chen, S. *et al.* (2015) Efficient production of marker-free transgenic 'Tarocco' blood orange (*Citrus sinensis* Osbeck) with enhanced resistance to citrus canker using a Cre/*loxP* site-recombination system. *Plant Cell, Tissue and Organ Culture*, **123**, 1–13.

Pereira, A.L., Carazzolle, M.F., Abe, V.Y., de Oliveira, M.L., Domingues, M.N., Silva, J.C. *et al.* (2014) Identification of putative TAL effector targets of the citrus canker pathogens shows functional convergence underlying disease development and defense response. *BMC Genomics*, **15**, 157.

Pires, N. & Dolan, L. (2010) Origin and diversification of basic-helix-loop-helix proteins in plants. *Molecular Biology and Evolution*, **27**, 862–874.

Qiang, X., Chen, L.-L., Ruan, X., Chen, D., Zhu, A., Chen, C. *et al.* (2013) The draft genome of sweet orange (*Citrus sinensis*). *Nature Genetics*, **45**, 59–66.

Rui, Y., Xiao, C., Yi, H., Kandemir, B., Wang, J.Z., Puri, V.M. *et al.* (2017) POLYGALACTURONASE INVOLVED IN EXPANSION3 functions in seedling development, rosette growth, and stomatal dynamics in *Arabidopsis* thaliana. *The Plant Cell*, **29**, 2413–2432.

Salmon-Divon, M., Dvinge, H., Tammoja, K. & Bertone, P. (2010) PeakAnalyzer: genome-wide annotation of chromatin binding and modification loci. *BMC Bioinformatics*, **11**, 415.

Schröder, F., Lisso, J., Lange, P. & Müssig, C. (2009) The extracellular EXO protein mediates cell expansion in *Arabidopsis* leaves. *BMC Plant Biology*, **9**, 20.

Schwartz, A.R., Morbitzer, R., Lahaye, T. & Staskawicz, B.J. (2017) TALE-induced bHLH transcription factors that activate a pectate lyase contribute to water soaking in bacterial spot of tomato. *Proceedings of the National Academy of Sciences of the United States of America*, **114**, E897–E903.

Shuai, B., Reynaga-Peña, C. & Springer, P. (2002) The lateral organ boundaries gene defines a novel, plant-specific gene family. *Plant Physiology*, **129**, 747–761.

Šmehilová, M., Dobrůšková, J., Novák, O., Takáč, T. & Galuszka, P. (2016) Cytokinin-specific glycosyltransferases possess different roles in cytokinin homeostasis maintenance. *Frontiers in Plant Science*, **7**, 1264.

Soprano, A.S., Giuseppe, P.O.D., Shimo, H.M., Lima, T.B. & Benedetti, C.E. (2017) Crystal structure and regulation of the citrus Pol III repressor MAF1 by auxin and phosphorylation. *Structure*, **25**, 1360–1370.

Soprano, S.A., Abe, Y.V., Smetana, C.H.J. & Benedetti, E.C. (2013) Citrus MAF1, a repressor of RNA polymerase III, binds the *Xanthomonas citri* canker elicitor PthA4 and suppresses citrus canker development. *Plant Physiology*, **163**, 232–242.

Su, J., Zhang, M., Zhang, L., Sun, T., Liu, Y., Lukowitz, W. *et al.* (2017) Regulation of stomatal immunity by interdependent functions of a pathogen-responsive MPK3/MPK6 cascade and abscisic acid. *The Plant Cell*, **29**, 526–542.

Swarup, S., Feyter, R.D., Brlansky, R.H. & Gabriel, D.W. (1991) A pathogenicity locus from *Xanthomonas citri* enables strains from several pathovars of *X. campestris* to elicit cankerlike lesions on citrus. *Phytopathology*, **81**, 256–257.

Swarup, S., Yang, Y., Kingsley, M.T. & Gabriel, D.W. (1992) An *Xanthomonas citri* pathogenicity gene, pthA, pleiotropically encodes gratuitous avirulence on nonhosts. *Molecular Plant-Microbe Interactions*, **5**, 204–213.

Thatcher, L.F., Powell, J.J., Aitken, E.A.B., Kazan, K. & Manners, J.M. (2012) The lateral organ boundaries domain transcription factor LBD20

functions in fusarium wilt susceptibility and jasmonate signaling in *Arabidopsis*. *Plant Physiology*, **160**, 407–418.

Thimm, O., Blasing, O., Gibon, Y., Nagel, A., Meyer, S., Kruger, P. *et al.* (2010) MAPMAN: a user-driven tool to display genomics data sets onto diagrams of metabolic pathways and other biological processes. *The Plant Journal*, **37**, 914–939.

Uluisik, S. & Seymour, G.B. (2020) Pectate lyases: their role in plants and importance in fruit ripening. *Food Chemistry*, **309**, 125559.

Wang, X., Zhang, S., Su, L., Liu, X. & Hao, Y. (2013) A genome-wide analysis of the LBD (LATERAL ORGAN BOUNDARIES domain) gene family in *Malus domestica* with a functional characterization of *MdLBD11*. *PLoS One*, **8**, e57044.

Xu, C., Cao, H., Zhang, Q., Wang, H., Xin, W., Xu, E. *et al.* (2018) Control of auxin-induced callus formation by bZIP59-LBD complex in *Arabidopsis* regeneration. *Nature Plants*, **4**, 108–115.

Xu, C., Luo, F. & Hochholdinger, F. (2016) LOB domain proteins: beyond lateral organ boundaries. *Trends in Plant Science*, **21**, 159–167.

Yan, Q. & Wang, N. (2012) High-throughput screening and analysis of genes of *Xanthomonas citri* subsp. *citri* involved in citrus canker symptom development. *Molecular Plant-Microbe Interactions*, **25**, 69–84.

Yang, L., Hu, C., Li, N., Zhang, J., Yan, J. & Deng, Z. (2011) Transformation of sweet orange [*Citrus sinensis* (L.) Osbeck] with *pthA-nls* for acquiring resistance to citrus canker disease. *Plant Molecular Biology*, **75**, 11–23.

Yordanov, Y.S., Regan, S. & Busov, V. (2010) Members of the LATERAL ORGAN BOUNDARIES DOMAIN transcription factor family are involved in the regulation of secondary growth in *Populus*. *The Plant Cell*, **22**, 3662–3677.

Zhang, D. & Zhang, B. (2020) Pectin drives cell wall morphogenesis without turgor pressure. *Trends in Plant Science*, **25**, 719–722.

Zhang, J., Huguet-Tapia, J.C., Hu, Y., Jones, J., Wang, N., Liu, S. *et al.* (2017) Homologues of CsLOB1 in citrus function as disease susceptibility genes in citrus canker. *Molecular Plant Pathology*, **18**, 798–810.

Zhang, L.-Y., Bai, M.-Y., Wu, J., Zhu, J.-Y., Wang, H., Zhang, Z. *et al.* (2009) Antagonistic HLH/bHLH transcription factors mediate brassinosteroid regulation of cell elongation and plant development in rice and *Arabidopsis*. *The Plant Cell*, **21**, 3767–3780.

Zhang, Y., Li, Z., Ma, B., Hou, Q. & Wan, X. (2020) Phylogeny and functions of LOB domain proteins in plants. *International Journal of Molecular Sciences*, **21**, 2278.

Zou, X., Long, J., Zhao, K., Peng, A., Chen, M., Long, Q. *et al.* (2019) Overexpressing GH3.1 and GH3.1L reduces susceptibility to *Xanthomonas citri* subsp. *citri* by repressing auxin signaling in citrus (*Citrus sinensis* Osbeck). *PLoS One*, **14**, e0220017.

Zou, X., Peng, A., Xu, L., Liu, X., Lei, T., Yao, L. *et al.* (2013) Efficient auto-excision of a selectable marker gene from transgenic citrus by combining the Cre/*loxP* system and ipt selection. *Plant Cell Reports*, **32**, 1601–1613.

Zou, X., Song, E., Peng, A., He, Y., Xu, L., Lei, T. *et al.* (2014) Activation of three pathogen-inducible promoters in transgenic citrus (*Citrus sinensis* Osbeck) after *Xanthomonas axonopodis* pv. *citri* infection and wounding. *Plant Cell, Tissue and Organ Culture*, **117**, 85–98.

报告编号：202109-257

检 索 报 告

项目名称：论文被 SCI 收录情况

委 托 人：西南大学柑桔研究所　　邹修平

日　　期：2021 年 09 月 22 日

认证单位：教育部科技查新工作站 N08

二 O 二 O 年制

6	通讯作者	Transcription factor WRKY22 regulates canker susceptibility in sweet orange (Citrus sinensis Osbeck) by enhancing cell enlargement and CsLOB1 expression	000624975000013	IF_{2020}=6.793	中科院类别基础版 分区 小类 GENETICS & HEREDITY 遗传学 1区 小类 HORTICULTURE 园艺 1区 小类 PLANT SCIENCES 植物科学 1区 大类 农林科学 1区	2021	英文	国外
7	1	CsLOB1 regulates susceptibility to citrus canker through promoting cell proliferation in citrus	000631375400001	IF_{2020}=6.417	中科院类别基础版 分区 小类 PLANT SCIENCES 植物科学 1区 大类 生物 2区	2021	英文	国外